University of Groningen

Inputs of iron, manganese and aluminium to surface waters of the Northeast Atlantic Ocean and the European continental shelf

Jong, Jeroen T.M. de; Boyé, Marie; Gelado-Caballero, Maria D.; Timmermans, Klaas R.; Veldhuis, Marcel J.W.; Nolting, Rob F.; Berg, Constant M.G. van den; de Baar, Henricus

IMPORTANT NOTE: You are advised to consult the publisher's version (publisher's PDF) if you wish to cite from it. Please check the document version below.

Document Version
Publisher's PDF, also known as Version of record

Link to publication in University of Groningen/UMCG research database

ELSEVIER

Inputs of iron, manganese and aluminium to surface waters of the Northeast Atlantic Ocean and the European continental shelf

Jeroen T.M. de Jong [a],*, Marie Boyé [b,1], Maria D. Gelado-Caballero [c],
Klaas R. Timmermans [a], Marcel J.W. Veldhuis [a], Rob F. Nolting [a],
Constant M.G. van den Berg [b], Hein J.W. de Baar [a]

[a] *Royal Netherlands Institute for Sea Research (NIOZ), PO Box 59, 1790 AB Den Burg, Texel, The Netherlands*
[b] *Oceanography Laboratories, University of Liverpool, Liverpool L69 3BX, United Kingdom*
[c] *Facultad de Ciencias del Mar, University of Las Palmas de Gran Canaria, 35017 Las Palmas, Spain*

Abstract

Dissolved Fe, Mn and Al concentrations (dFe, dMn and dAl hereafter) in surface waters and the water column of the Northeast Atlantic and the European continental shelf are reported. Following an episode of enhanced Saharan dust inputs over the Northeast Atlantic Ocean prior and during the cruise in March 1998, surface concentrations were enhanced up to 4 nmol L^{-1} dFe, 3 nmol L^{-1} dMn and 40 nmol L^{-1} dAl and returned to 0.6 nmol L^{-1} dFe, 0.5 nmol L^{-1} dMn and 10 nmol L^{-1} dAl towards the end of the cruise three weeks later. A simple steady state model (MADCOW, [Measures, C.I., Brown, E.T., 1996. Estimating dust input to the Atlantic Ocean using surface water aluminium concentrations. In: Guerzoni. S. and Chester. R. (Eds.), The impact of desert dust across the Mediterranean, Kluwer Academic Publishers, The Netherlands, pp. 301–311.]) was used which relies on surface ocean dAl as a proxy for atmospheric deposition of mineral dust. We estimated dust input at 1.8 g m^{-2} yr^{-1} (range 1.0–2.9 g m^{-2} yr^{-1}) and fluxes of dFe, dMn and dAl were inferred. Mixed layer steady state residence times for dissolved metals were estimated at 1.3 yr for dFe (range 0.3–2.9 yr) and 1.9 yr for dMn (range 1.0–3.8 yr). The dFe residence time may have been overestimated and it is shown that 0.2–0.4 yr is probably more realistic. Using vertical dFe versus Apparent Oxygen Utilization (AOU) relationships as well as a biogeochemical two end member mixing model, regenerative Fe:C ratios were estimated respectively to be 20±6 and 22±5 µmol Fe:mol C. Combining the atmospheric flux of dFe to the upper water column with the latter Fe:C ratio, a 'new iron' supported primary productivity of only 15% (range 7%–56%) was deduced. This would imply that 85% (range 44–93%) of primary productivity could be supported by regenerated dFe. The open ocean surface data suggest that the continental shelf is probably not a major source of dissolved metals to the surface of the adjacent open ocean. Continental shelf concentrations of dMn, dFe, and to a lesser extent dAl, were well correlated with salinity and express mixing of a fresher continental end member with Atlantic Ocean water flowing onto the shelf. This means probably that diffusive benthic fluxes did not play a major role at the time of the cruise.
© 2007 Elsevier B.V. All rights reserved.

Keywords: Sea water; Trace metals; Eolian dust; Oceans; Continental shelves; Atlantic

* Corresponding author. Present address: Département des Sciences de la Terre et de l'Environnement, Université Libre de Bruxelles (ULB) CP 160/02, Avenue F. D. Roosevelt 50, B-1050, Brussels, Belgium. Tel.: +32 2 6502236.
E-mail address: jdejong@ulb.ac.be (J.T.M. de Jong).

[1] Present address: Laboratoire des Sciences de l'Environnement Marin (LEMAR), CNRS-UMR 6539, Institut Universitaire Européen de la Mer (IUEM), Technopole Brest-Iroise, Place Nicolas Copernic, 29280 Plouzané, France.

1. Introduction

Iron and manganese are well known to be essential trace nutrients to marine phytoplankton, playing a key role as enzymatic cofactors in cell metabolism, e.g. N_2 fixation, nitrate assimilation and photosynthesis. Aluminium has so far not been shown to have a biological function, but its association to phytoplankton has been observed, either by incorporation into diatom frustules or by surface adsorption (e.g. Gehlen et al., 2002; Moran and Moore, 1992; Van Bennekom et al., 1991; Moran and Moore, 1988). Despite the high crustal abundance of aluminium (7.96%), iron (4.32%) and manganese (0.0716%) (Wedepohl, 1995), their dissolved concentrations in the modern ocean are at extremely low levels of nanomoles per liter or less, due to their low solubility in oxygenated seawater. It is widely accepted that the low availability of Fe influences the carbon cycle in large parts of the ocean by limiting primary productivity (e.g. Boyd et al., 2000; Coale et al., 1996, Martin et al., 1991). The impact of iron on primary productivity in the oceans would depend on the amount and speciation of the supplied iron, and taxa-specific bioavailability (Hutchins et al., 1999). It has been hypothesized that iron supply to the oceans could have played a crucial role in global climate changes of the past (Martin, 1990).

Atmospheric supply to the surface ocean can be an important source of Fe, Mn and Al (Jickells and Spokes, 2001; De Baar and De Jong, 2001; Duce et al., 1991; Duce and Tindale, 1991), particularly dominant downwind of large arid landmasses such as the subtropical East Atlantic Ocean under the Saharan dust plume. The impact of atmospheric input to the surface ocean would depend on the chemical composition of the aerosol, its exposure time to atmospheric conditions (sunlight, acidic cloud chemistry), its deposition mode (wet or dry) (Jickells and Spokes, 2001) and solution phase removal of the solubilized constituents upon deposition in seawater (Spokes and Jickells, 1996).

Our understanding of the complex interactions between aerosol and the surface ocean is still incomplete to date, mainly due to undersampling and analytical difficulties. This paper presents a high-resolution surface and vertical data set of dissolved Fe, Mn and Al along transects covering a range of marine environments (Strait of Dover, English Channel, continental shelf of the Celtic Sea and the open Northeast Atlantic Ocean). Dissolved aluminium has received attention as a tracer of terrigenous input to the oceans and has been used in a simple model by Measures and Brown (1996) and Measures and Vink (2000) to obtain estimates for atmospheric dust inputs to the surface ocean. We applied this

model to our data to calculate the atmospheric dust flux and associated fluxes of iron, manganese and aluminium to the Northeast Atlantic Ocean. The biogeochemical implication of these atmospheric fluxes on the surface mixed layer of the Northeast Atlantic is discussed. We have also attempted to identify sources of dissolved metals on the continental shelf.

2. Materials and methods

2.1. Sampling

Seawater samples from the sea surface and water column were collected during cruise MERLIM98 (Marine Ecosystem Regulation by LIMitation of carbon dioxide and trace metals), in early spring (March 2 until March 27, 1998) on board of the Dutch research vessel '*Pelagia*' (cruise 64PE114). After leaving the North Sea under adverse weather conditions, the sampling program started for dFe measurement on March 6 just after the continental shelf break was crossed. While steaming in southwest direction the 23°W meridian was reached on March 10 (transect I). Further transects were sampled along 23°W between 37°N and 45°N (transects II–VI). The return cruise track (transects VII–VIII) started March 20 at 37°N, 23°W and went first north and then northeastward across the continental shelf in the Goban Spur area into the English Channel and the North Sea until 51°N, 2°W on March 26. Larger surface samples for dFe and additional dMn and dAl, were only taken during the return transect due to the limited availability of sufficiently sized clean sample bottles on board. Two shallow stations (0–200 m) were sampled during the outbound transect, while four deep stations (sampled in a shallow cast 0–200 m followed by a deep cast 200–2000 m) were occupied along 23°W between 37°N and 42.5°N. See Fig. 1 and Appendices A and B for cruise track and station positions.

Surface seawater was collected by a tow-fish deployed about 1 m below the surface and a few meters away from the hull while steaming at 8 to 11 knots. Seawater was pumped up through acid cleaned braided PVC tubing by a peristaltic pump, at a flow rate of 1 L min^{-1} and filtered through a Sartorius Sartobran P filter cartridge (polypropylene housing, cellulose acetate filter 0.2 μm porosity with internal 0.45 μm pre-filter) under class 100 clean air conditions.

Water column seawater samples were collected with pre-cleaned, Teflon coated PVC Go-Flo samplers (General Oceanics, Miami, USA) deployed on a Kevlar cable. Go-Flo's were closed by tripping with Teflon messengers. The collected seawater samples were filtered in-line
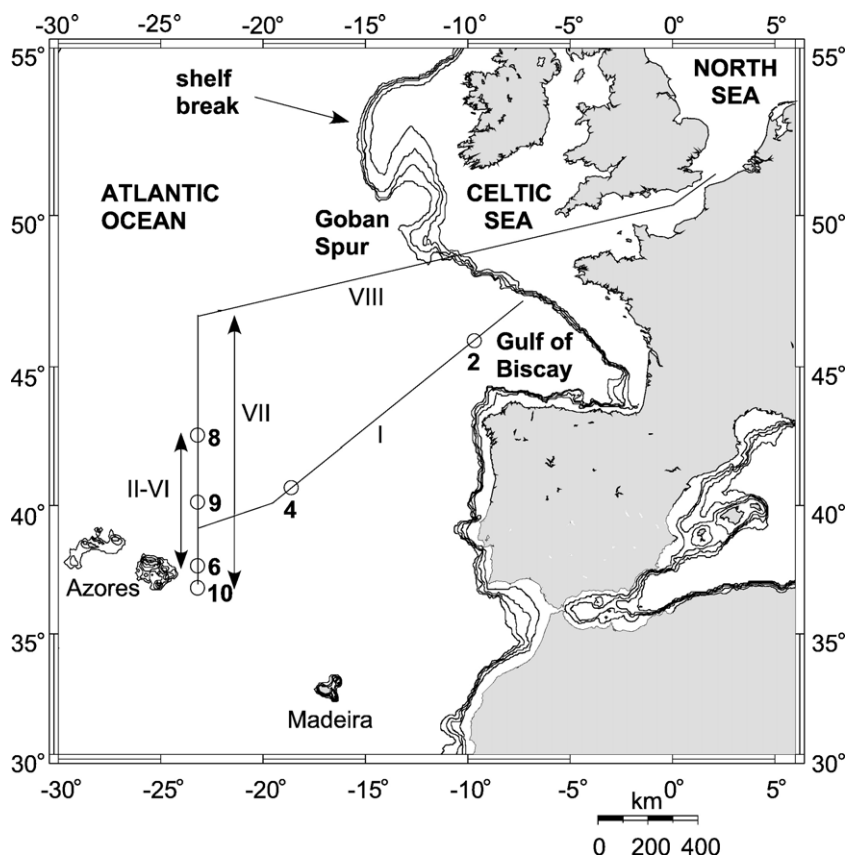
Fig. 1. Map of the MERLIM98 cruise transects with station locations.

through cleaned polycarbonate 0.2 μm membrane filters (Poretics, 47 mm diameter) in Teflon filter holders under moderate nitrogen overpressure (0.3–0.5 bar).

As the analytical technique for iron required it to be in the Fe(III) form, caution was taken to keep the samples in the dark at room temperature for minimally one hour to ensure the oxidation of any present Fe(II) in the absence of photochemical reduction. After this step the samples were acidified to pH = 1.8 with triple sub-boiled concentrated nitric acid (1 ml L^{-1}) and measured minimally 2 h upon acidification. Mn and Al were analyzed in the same sample bottles back in the home laboratory shortly after the cruise.

2.2. Analytical methods

2.2.1. Trace metals

dFe, dMn and dAl were measured by various adaptations of existing flow injection analytical techniques (FIA) with in-line pre-concentration on a column of immobilized 8-hydroxyquinoline chelating resin (TSK-8HQ, Landing et al., 1986). The method of standard additions was applied. Blanks were determined by com-

paring single and double additions of acids and buffers to a sample of low trace metal seawater, while also accounting for a 1 minute UHP water column rinse time. Our methods are described in more detail in De Jong et al. (2000, 1998) and will be only briefly summarized in the following paragraphs.

Fe-FIA-CL: the measurement of Fe is based on the chemiluminescence produced by the iron mediated oxidation of luminol by hydrogen peroxide (Obata et al., 1993). The acidified seawater sample was buffered in-line by addition of clean ammonium acetate buffer to obtain a final pH of ~4.0. We found total blanks and detection limits (3σ of the blank) of 0.04 ± 0.04 nmol L^{-1} (*n* = 4) and 0.11 nmol L^{-1} respectively. Precision (1σ) was typically around 2% at the 0.5 nmol L^{-1} level.

Al-FIA-FL: Aluminium concentrations were determined using a FIA adaptation of the fluorometric lumogallion technique (Resing and Measures, 1994). Prior to analysis, sample aliquots of 100 ml filtered acidified seawater in LDPE bottles were buffered by manual addition of clean ammonium acetate buffer to obtain a final pH of 5.5 for in-line pre-concentration.

Typical precision was 2% at the 10 nmol L^{-1} level, the blank was 0.31 ± 0.23 nmol L^{-1}, ($n=4$) and the detection limit 0.69 nmol L^{-1}.

Mn-FIA-VIS: Manganese concentrations were determined by spectrophotometry via the manganese mediated oxidation of Tiron by hydrogen peroxide in the presence of 2,2′-bipyridyl (Mallini and Shiller, 1993). The pre-concentration pH was set to 8.0 ± 0.2 using clean, saturated TRIS buffer in 100 ml aliquots of acidified seawater. Blanks and detection limits were 0.05 ± 0.03 nmol L^{-1} ($n=7$) and 0.09 nmol L^{-1} respectively. Precision was around 2% at the 0.5 nmol L^{-1} level.

2.2.2. Analytical accuracy trace metals

The accuracy of the Fe-FIA-CL and Mn-FIA-VIS systems was checked by analyzing NASS-4, NASS-5 and CASS-3 reference seawater from the National Research Council of Canada. All results were in good agreement with the certified values: NASS-4 Fe 1.90 ± 0.21 nmol L^{-1} ($n=7$) (certified 1.88 ± 0.29 nmol L^{-1}), Mn 7.04 ± 0.28 nmol L^{-1} ($n=4$) (certified 6.92 ± 0.43 nmol L^{-1}); NASS-5 Fe 3.35 ± 0.51 nmol L^{-1} ($n=8$) (certified 3.71 ± 0.63 nmol L^{-1}), Mn 18.28 ± 0.78 nmol L^{-1} ($n=2$) (certified 16.7 ± 1.0 nmol L^{-1}); CASS-3: Fe 24.9 ± 0.7 nmol L^{-1} ($n=2$) (certified 22.6 ± 3.0 nmol L^{-1}), Mn 44.9 ± 4.3 nmol L^{-1} ($n=2$) (certified 45.7 ± 6.6 nmol L^{-1}) (De Jong et al., 2000). These reference materials are not certified for Al, unfortunately. The analytical merit of the Al-FIA-FL method was however reflected in the good agreement of our vertical dAl data with data from nearby stations from Measures (1995) who used solvent extraction/gas chromatography and from Kramer et al. (2004) using Al-FIA-FL. The solvent extraction/gas chromatography technique from Measures (1995) had been intercalibrated in the past with the lumogallion batch method, showing good agreement (Measures et al., 1986).

2.2.3. Additional parameters

Concentrations of the nutrients nitrate, phosphate, silicate and ammonium were determined in filtered seawater using TRAACS 800 auto-analyzers following established methods (Grasshoff et al., 1983).

For chlorophyll a, seawater was filtered on Whatman glass fiber filters (GF/F, 47mm), which were stored at -80 °C for later analysis. After extraction in methanol, Chl a was measured by a Turner Design fluorimeter.

Phytoplankton composition was determined applying flow cytometry (Coulter Electronics, XL-MCL) (Veldhuis and Kraay, 2004). Samples were directly measured on board and analyzed using the standard software package. *Synechococcus*-type of picophytoplankton could be discriminated from other phytoplankton by the presence of the pigment phyco-erythrin.

3. Results

3.1. Hydrography

The large-scale hydrographical structures encountered during this expedition were (1) European shelf waters characterized by low temperatures and salinity rapidly increasing in southwest direction toward the shelf break, and (2) Eastern North Atlantic Central Water (ENACW) with a linear gradient of increasing salinity and temperature toward the south, typical of subtropical gyre waters (Fig. 2A–B). On transect VII a weak frontal system was encountered while steaming to the north between 41.5°N and 42.5°N at 23°W, where salinity dropped from 36 to 35.8 and temperature from 15 to 14 °C. This front forms probably the boundary between the northeastward flowing North Atlantic Current (NAC) and waters proper to the North Atlantic gyre.

The upper water column structure in the northern part of the study area (station 2) was characterized by a deep thermocline at 150 m due to deep winter convection. More to the south, the thermocline was at 75 to 100 m at stations 4 and 6, but shoaled to 50, 40 and 50 m at stations 8, 9 and 10 respectively. Below 200 m until about 900 m North Atlantic Central Water (NACW) is present. Underlying the NACW is the high salinity Mediterranean Outflow Water (MOW) between around 800–1100 m. Its salinity signature from CTD profiles (not shown) generally decreases in northward direction from 35.65 (station 10) to 35.53 (station 8). Below the MOW a mix of North Atlantic Deep Water and Labrador Seawater (LSW) is found.

3.2. Biology

Transect I chlorophyll a concentrations (Fig. 2F) gradually increased southward from 0.3–0.4 µg L^{-1} at the continental shelf until a broad maximum of 0.6–0.8 µg L^{-1} between 45.5°N and 39.5°N, south of which it dropped to values as low as 0.2 µg L^{-1}. The return transects VII and VIII showed a general small increase compared with transect I, although the distribution pattern had become patchy with peaks in the range of 1–1.7 µg L^{-1}. The highest Chl a peak of 1.7 µg L^{-1} at 46°N coincided with a drop in nutrients, including silicate and this may have been indicative of the occurrence of a diatom bloom. This was not observed in terms of cell numbers, either because diatom cells may have
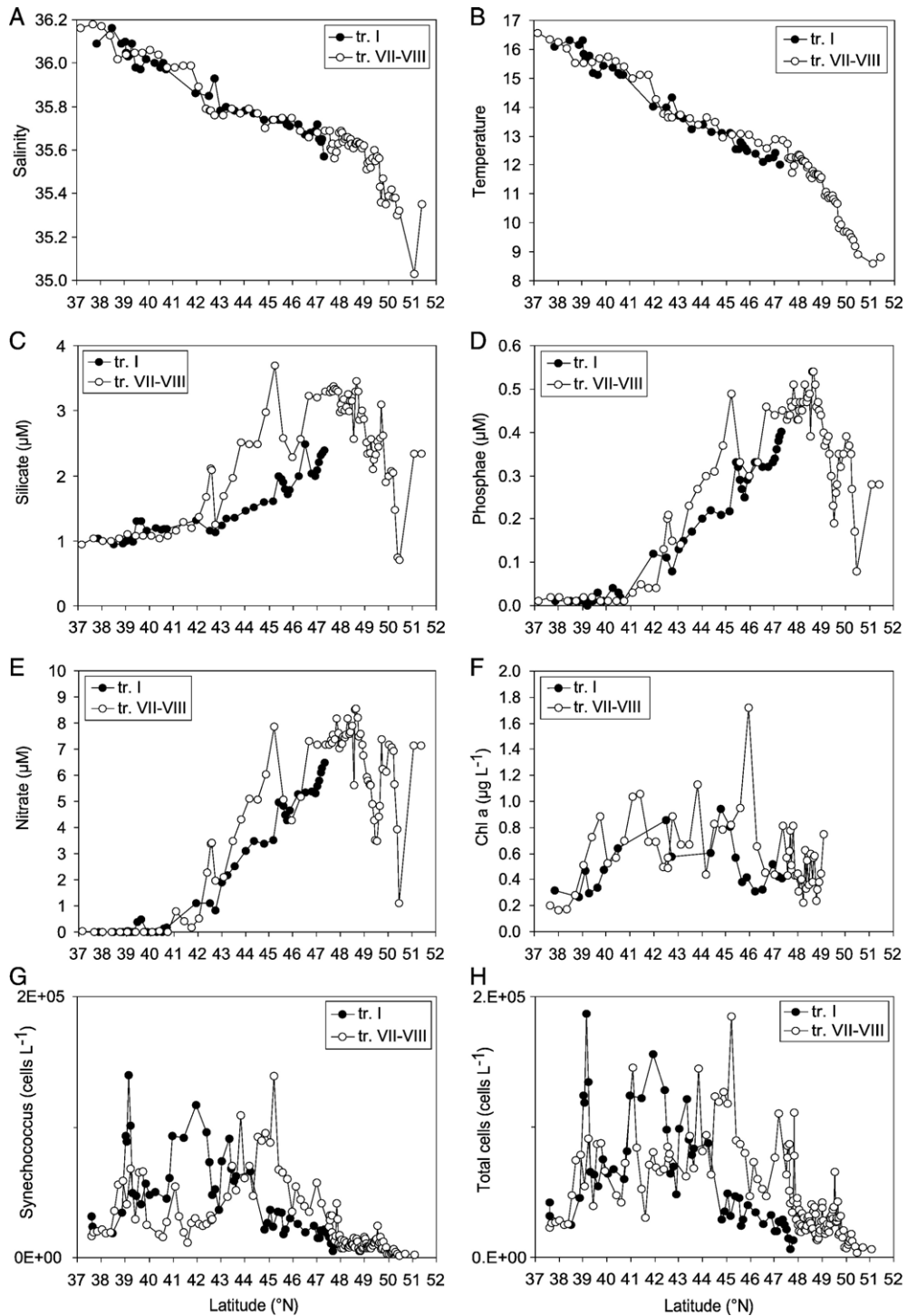
Fig. 2. Transect parameters A) salinity (‰), B) temperature (°C), C) silicate (μmol L^{-1}), D) phosphate (μmol L^{-1}), E) nitrate (μmol L^{-1}), F) Chlorophyll a (μg.L^{-1}), G) *Synechococcus* cell numbers (cells ml^{-1}), H) total cell numbers (cells ml^{-1}).

been too large (>10 μm) for detection by flow cytometry, or because the higher relative chlorophyll fluorescence of large eukaryotes in combination with low numbers of large cells may have led to slight discrepancies between cell abundance distribution and Chl a distribution.

The composition of the phytoplankton community in the surface waters (Fig. 2G–H) was dominated by picophytoplankton (<2 μm in size). Usually less than 5% of the population consisted of eukaryotic species larger than 5 μm. Of the picophytoplankton population, the prokaryote *Synechococcus* numerically dominated this algal group (60% to 80% of cell numbers). Although we lack size-fractionated biomass data, a recent indication of the general importance of the picophytoplankton community can be found in Teira et al. (2005). Based on a multi-year large-scale survey of this ocean region, they estimated a 71% contribution to phytoplankton biomass and a 54% contribution to primary productivity. Albeit much less abundant, it must be noted that picoeukaryotes may still have represented a substantial fraction of this picophytoplankton biomass (Maranon et al., 2003; Zubkov et al., 1998).

3.3. Surface trace metal concentrations

Three different surface water regions (Fig. 3A–D) were defined based on water depth and distinct trace metal signatures: (1) open ocean (water depth >250 m), (2) continental shelf waters (water depth 100–250 m) and (3) coastal sea (water depth <100 m). Average surface concentration ($\pm 1\sigma$) of dFe during open ocean

transect I shortly after the beginning of the transect was high at 1.85 ± 0.76 nmol L^{-1} Fe ($n=24$). The rest of open ocean transect I and transects II–VI had lower dFe concentrations of 0.93 ± 0.38 nmol L^{-1} Fe ($n=43$). During transects VII and the oceanic part of transect VIII dissolved concentrations were as follows: 0.61 ± 0.17 nmol L^{-1} Fe ($n=51$), 0.50 ± 0.08 nmol L^{-1} Mn ($n=47$) and 10.7 ± 1.8 nmol L^{-1} Al ($n=44$). On the continental shelf of the Celtic Sea, dissolved concentrations had increased to 1.21 ± 0.35 nmol L^{-1} Fe ($n=10$), 1.10 ± 0.32 nmol L^{-1} Mn ($n=10$) and 14.9 ± 8.1 nmol L^{-1} Al ($n=10$). Coastal sea concentrations in waters comprising the English Channel, the Strait of Dover and the Southern Bight of the North Sea, were 2.4 ± 1.4 nmol L^{-1} Fe ($n=15$), 2.4 ± 1.0 nmol L^{-1} Mn ($n=15$) and 33 ± 10 nmol L^{-1} Al ($n=15$). The concentrations reported in this study are comparable with previously published data, see Table 1.

3.4. Vertical trace metal concentrations

Generally, dFe (Fig. 4) showed nutrient type profiles for all stations with surface mixed layer values of 1.04 ± 0.29 nmol L^{-1} ($n=28$). This is consistent with the surface concentrations measured between the stations on transects II–VI, 0.93 ± 0.38 nmol L^{-1} Fe ($n=43$). One
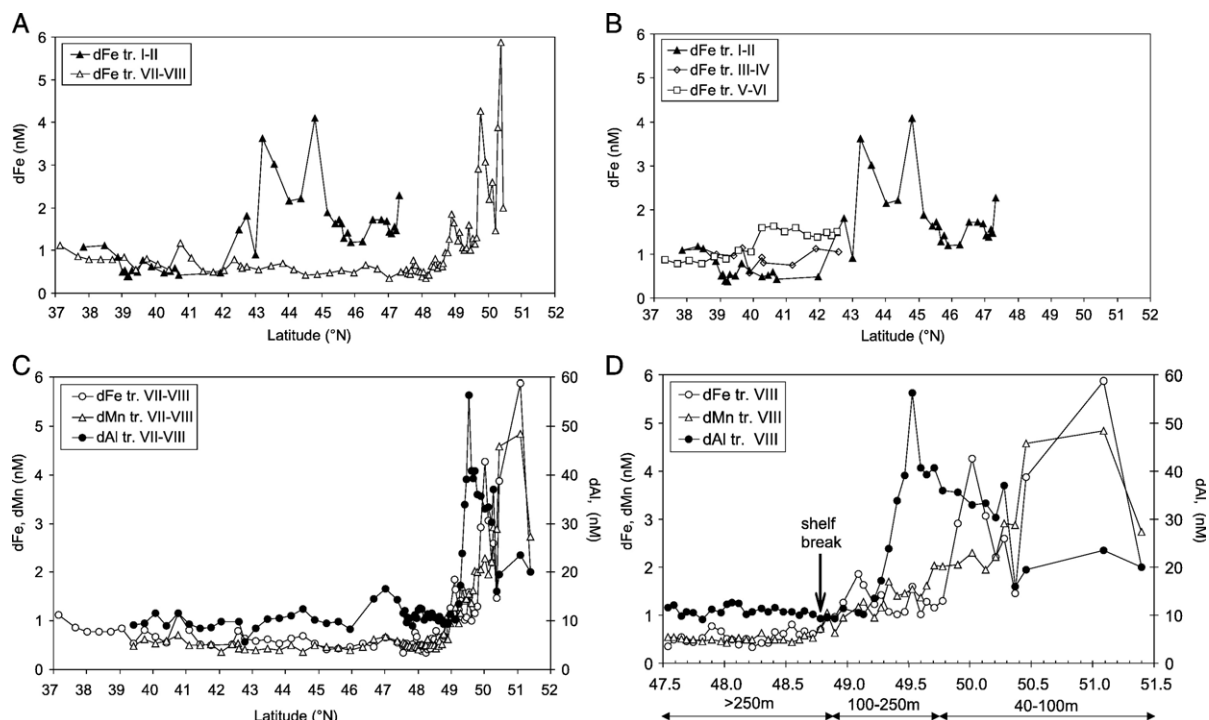

Fig. 3. Surface trace metal data: A) dFe transects I–II and VII–VIII, B) dFe transects I–VI, C) dFe, dMn, dAl transects VII–VIII, D) as C, blown up section of approach and crossing of continental shelf break.

Table 1
Literature comparison of MERLIM98 trace metal data

Area	Time period	Fe (nM)	Mn (nM)	Al (nM)	Filtration	Reference
Northeast Atlantic	March 1998	2.0±0.9 (25)	–	–	0.2 μm filtered	This work, Merlim98, transect I
	March 1998	0.9±0.4 (48)	–	–	0.2 μm filtered	This work, Merlim98, transects II–VI
	March 1998	0.7±0.3 (53)	0.5±0.1 (47)	11.0±2.6 (46)	0.2 μm filtered	This work, Merlim98, transects VII–VIII
	March 1998	0.8±0.2 (14)	–	–	0.2 μm filtered	Merlim98, transect VIII, Boyé et al. (2003)
	March–April 1982	–	0.7±0.3 (15)	11.4±3.3 (15)	Unfiltered	Cruise M60, Kremling (1985)
	May–June 1998	0.9±0.5 (44)	–	20.4±6.6 (16)	Unfiltered	Cruise AMT-6, Bowie et al. (2002)
	May 1990	–	–	8.8±3.4 (10)	Unfiltered	Cruise ANT VIII/7, Helmers and Rutgers van der Loeff (1993)
	September–October 1996	1.0±0.4 (16)	–	22.9±5.1 (11)	Unfiltered	Cruise AMT-3, Bowie et al. (2002)
	November 1990	–	–	5.7±1.4 (10)	Unfiltered	Cruise ANT IX/1, Helmers and Rutgers van der Loeff (1993)
Continental shelf	March 1998	1.2±0.4 (10)	1.1±0.3 (10)	14.9±8.1 (10)	0.2 μm filtered	This work, Merlim 98, transect VIII
	March 1998	1.1±0.1 (4)	–	–	0.2 μm filtered	Merlim98, transect VIII, Boyé et al. (2003)
	March–April 1982	–	1.6±0.7 (2)	20.9±2.5 (2)	0.4 μm filtered	Cruise M60, Kremling (1985)
	May–June 1998	1.0±0.4 (9)	–	11.9 (1)	unfiltered	Cruise AMT-6, Bowie et al. (2002)
English Channel	March 1998	2.4±1.4 (15)	2.4±1.0 (15)	33±10 (15)	0.2 μm filtered	This work, Merlim98, transect VIII
	March 1998	1.8±0.3 (6)	–	–	0.2 μm filtered	Merlim98, transect VIII, Boyé et al. (2003)
	March–April 1982	–	4.8±3.0 (10)	153±102 (10)	0.4 μm filtered	Cruise M60, Kremling (1985)
	May 1986	–	–	20±5 (48)	0.4 μm filtered	Hydes (1989)
	May 1986	–	3.8±2.1 (48)	–	0.4 μm filtered	Tappin et al. (1993)
	July 1984	–	6.5±1.7 (11)	8.8±3.1 (11)	0.4 μm filtered	Kremling and Hydes (1988)
	July–August 1986	–	5.0±3.0 (48)	–	0.4 μm filtered	Tappin et al. (1993)
	August 1986	–	–	10±4 (48)	0.4 μm filtered	Hydes (1989)
	November 1985	–	–	28±10 (48)	0.4 μm filtered	Hydes (1989)
	November–December 1985	–	2.3±0.7(48)	–	0.4 μm filtered	Tappin et al. (1993)

high value of 4.53 nmol L^{-1} at station 2, 10 m depth, was not used for calculating the mean. This sample was probably not contaminated, but influenced by a recent dust input event (see further below). Below the mixed layer dFe concentrations rose rapidly until at depths below 250 m dFe had steadied to deep water values of 1.65±0.19 nmol L^{-1} (n=31). Stations 8, 9 and 10 show a dFe minimum at around 30 m depth inside the Chl a maximum zone, this may have been a result of biological uptake and/or particle sorption.

Dissolved Mn concentrations (Fig. 4) exhibited typical scavenging type profiles with higher mixed layer values of 0.81±0.38 nmol L^{-1} (n=28) rapidly dropping to low deep water concentrations (>250 m) of

0.21±0.08 nmol L^{-1} (n=31). The somewhat large standard deviation of the average mixed layer concentrations of Mn is due to a continuous increase in southern direction. This could be consistent with the approach to the Saharan dust source as well as enhanced photoreduction from increased solar radiation towards the south. Dissolved Mn was high (3.13 nmol L^{-1}) at station 2, 10 m depth.

The profiles of dAl at stations 2 and 6 showed indication of enhanced atmospheric input with peaks of respectively 40.5 nmol L^{-1} and 21.4 nmol L^{-1} at 10 m depth (Fig. 4). The mean value of dAl (Fig. 4) in the surface mixed layer at all stations (except station 2) was 13.9±3.4 nmol L^{-1} (n=22). Below 250 m the
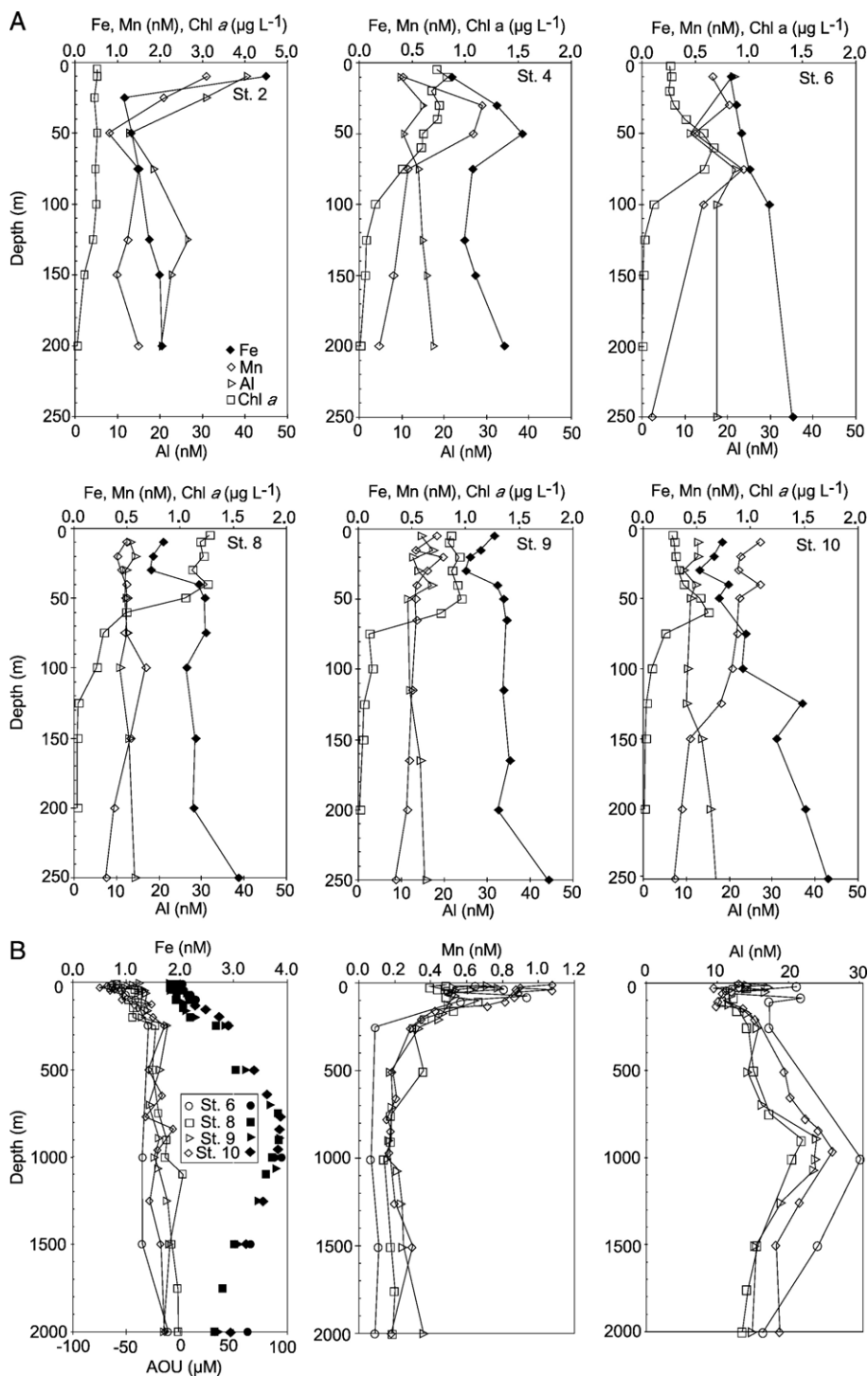
Fig. 4. A) vertical profiles dFe, dMn, dAl and Chl *a* upper 250 m. B) vertical profiles dFe, dMn, dAl and AOU, upper 2000 m.

concentrations steadily increased until the MOW, whose core between roughly 800–1100 m had average concentrations of 24.2±2.8 nmol L^{-1} (*n*=9). A closer look at the data reveals that dAl in the MOW decreases

in northern direction due to dilution of the high Al signature of the MOW: 25.9±3.4 nmol L^{-1} (stations 6 and 10, *n*=4) 23.8±0.2 nmol L^{-1} (station 9, *n*=3) and 21.4±0.9 nmol L^{-1} (station 8, *n*=2), stations 6 and 10

being more or less at the same geographical position facing the Strait of Gibraltar. Further to the south, Kramer et al. (2004) found similar maxima of 24 nmol L^{-1} at two stations in the core of the MOW at depths of 1000 m and 1300 m respectively. Measures (1995) found closer to the Strait of Gibraltar an Al maximum of 27 nmol L^{-1} in the MOW, at a depth of 1200 m.

4. Discussion

4.1. Dissolved Fe data quality assessment

With respect to the biogeochemical importance of iron a detailed data quality assessment is given below. In accompanying papers, Boyé et al. (2006, 2003) reported surface and deep iron concentrations measured by CSV during this cruise, that were similar compared to the FIA data presented here. These authors raised the issue that the vertical data were possibly too high as previous studies close to this ocean region have shown profiles with lower concentrations by 0.3–0.8 nmol L^{-1} (see Boyé et al. (2006) and references therein). Below it is argued from extensive testing of sampling and analytical devices, that the accuracy of the data was probably not compromised and that the data may be real.

(1) Samples from vertical profiles and a number of surface samples during the return transit were intercalibrated using the same sampling and filtration devices by CSV (Cathodic Stripping Voltammetry) and FIA with satisfactory result (see Table 1 and De Jong et al., 2000). This, together with the accurate results for reference seawater analyzed by FIA seem to exclude the possibility of a systematic analytical off-set.

(2) A possibility remains that CSV ≈ FIA may have been coincidental and that not all dFe was detected. For instance, dark storage of FIA samples before acidifying, in order to oxidize any present Fe(II), may not have been sufficient. This seems improbable in the light of the rapid oxidation kinetics of Fe(II). However, Bowie et al. (2006) reported that addition of hydrogen peroxide could increase for certain samples the detected concentration of Fe(III) by oxidation of still present reduced iron. These samples were acidified without a prior dark storage step though, so their acidification probably fixed the Fe(II) by slowing the oxidation rate at low pH. Boyé et al. (2003) found during this cruise open ocean Fe(II) exhibiting on average only 0.09 ± 0.11 nmol L^{-1} ($n=39$). This low level combined with the dark storage before acidifying, indicates that this potential loss factor probably did not play a role.

Another potential loss factor may have been insufficient acidification time at pH 1.8. This could have re-

sulted in some part of organic Fe or (in)organic colloidal Fe to escape detection. What instead has been detected would then reflect labile dFe and not total dFe. Recently however, Lohan et al. (2006) demonstrated that samples that were analyzed on board within 2 h upon collection had similar dFe concentrations as samples that were analyzed within 5 months. These authors found that after 1 h of acidification at pH 1.7 the dFe concentration reached a plateau of constant concentration. The conclusion therefore is that the acidification minimally 2 h before measurement is sufficient for detecting total dFe.

(3) Two in-line filtration methods were applied to GoFlo sampled vertical profiles of stations 9 and 10 (De Jong et al., 2000), namely membrane filtration (N$_2$-pressurized at 0.3–0.5 bar) and Sartorius Sartobran cartridge filtration (N$_2$-pressurized at 0.1 bar). The resulting essentially similar profiles reflect the absence of filtration artifacts.

(4) Data from different surface sampling techniques: GoFlo sampling for the surface mixed layer at the stations (1.04 ± 0.29 nmol L^{-1}, $n=28$) and underway surface sampling between the stations (0.93 ± 0.38 nmol L^{-1}, $n=43$), agreed well. Additionally, two underway surface sampling techniques were tested simultaneously on a short transect: filling bottles from a rubber boat followed by filtering them back on board (0.99 ± 0.08 nmol L^{-1}, rsd = 8%, $n=4$) and tow-fish sampling (0.97 ± 0.02 nmol L^{-1}, rsd = 2%, $n=5$). The similarity of these results suggests the absence of sampling artifacts.

(5) Inadvertent contamination at any step during the sampling and analytical process was deemed to be under control, as this would have led to highly spurious profiles for all of the trace metals here analyzed, instead of the oceanographically consistent vertical profiles that were obtained.

It should be pointed out that high deep dFe values are not unusual in the Northeast Atlantic under the Saharan dust plume, for instance Bergquist and Boyle (2006): up to 1.2 nmol L^{-1} between 130–1050 m at 10°N, 45°W; Landing et al. (2003): up to 2.3 nmol L^{-1} between 100–1000 m at 5°–18°N, 20°W, Ussher et al. (2006): up to 1.5 nmol L^{-1} between 50–200 m at 0°–20°N, 20°W. The occurrence of unusually high dust deposition events over this ocean region (Torres-Padron et al., 2002) prior to and during the beginning of this cruise (see also next paragraph) could have been responsible for not only enhancing surface dFe concentrations but also increasing dFe at greater depth, at least until 2000 m depth. During these episodic and transient non-steady state periods, rapidly sinking mineral dust particles, as well as mineral and biogenic iron associated with phytodetritus aggregates (Hamm, 2002; Ittekkot, 1993), could have been
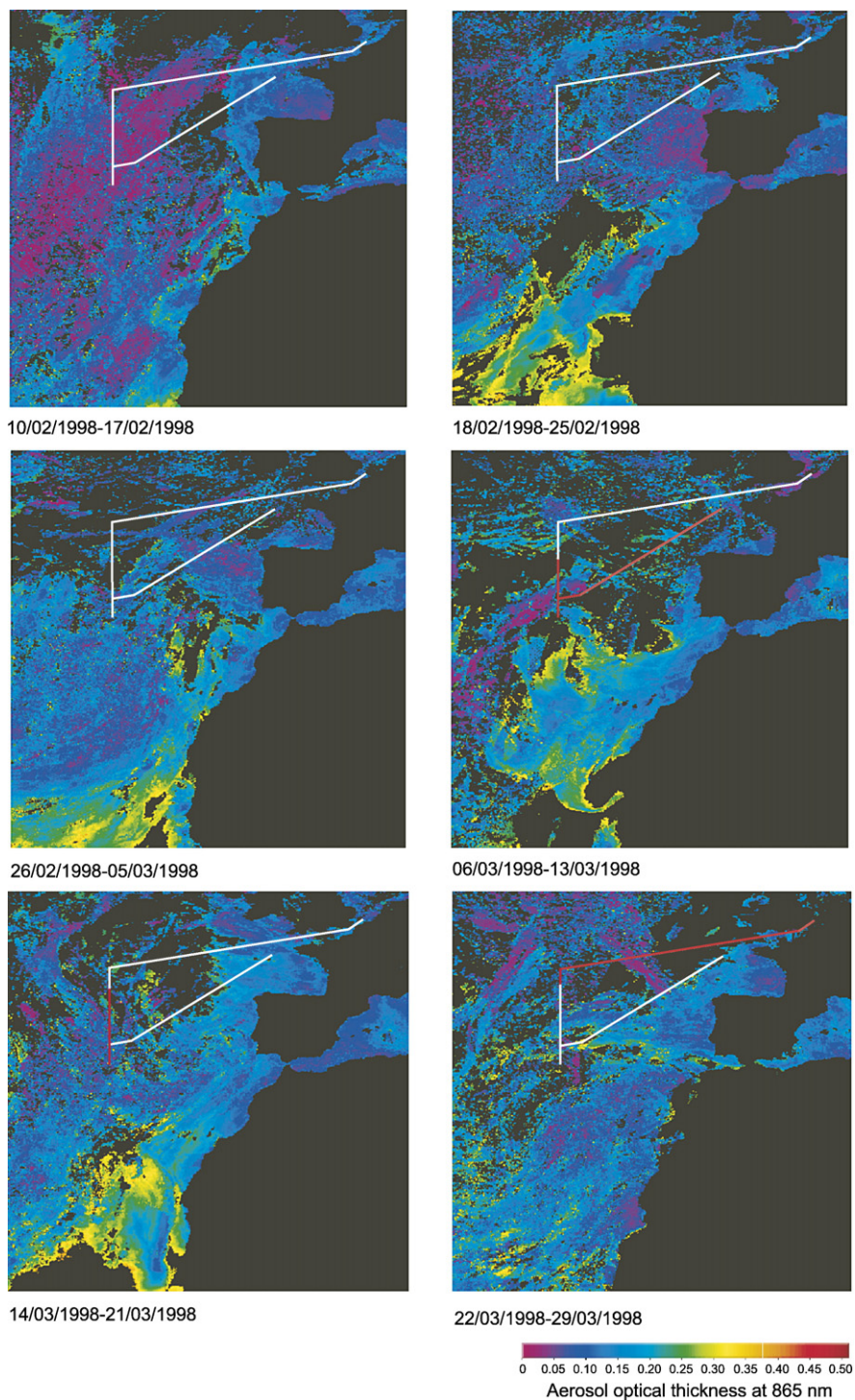
Fig. 5. Dust over the Northeast Atlantic Ocean during February and March 1998 (dd.mm.yy): SeaWiFS (Sea-viewing Wide Field of view Sensor) aerosol optical thickness (Tau 865 nm), weekly averages. Indicated as a white line is the surface transect between March 6 and March 26, 1998, while indicated in red is the presence of the ship on the transect during the covered period.

responsible for higher dFe by continued iron dissolution driven by organic ligands (Boyé et al., 2006) and remineralization (Bergquist and Boyle, 2006), while being exported to greater depth.

4.2. Surface transects

4.2.1. Transects I–VI: Northeast Atlantic Ocean

During February and March 1998 SeaWiFS Tau (865 nm) aerosol optical thickness remote sensing (Fig. 5) revealed dust outbreak activity above the Northeast Atlantic ocean and was particularly high during the second half of February 1998 and the first half of March 1998. The development of aerosol concentrations was monitored on the island of Gran Canaria (28°N, 16.5°W), where dust pulses occurred on February 12 (1300 µg m^{-3}), February 27 (1100 µg m^{-3}), March 6, (180 µg m^{-3}) and March 9, 1998 (270 µg m^{-3}) (Fig. 6). *Forward* air mass trajectories (Fig. 7) obtained with the HYSPLIT dispersion model (Draxler and Rolph, 2003), available from the U.S. National Oceanic and Atmospheric Administration (NOAA), indicated that the high dust that occurred above the Canary Islands in February 1998 and on March 6, 1998 could indeed have been transported across our research area.

Directly after the start of the measurement program on March 6, unexpectedly high dFe concentrations from 1.5 nmol L^{-1} up to 4.1 nmol L^{-1} were found in a broad zone from 47°N until 43°N (Fig. 3A). These high dFe concentrations in waters off the continental shelf were weakly correlated with salinity (Fig. 8A). The enhanced Fe concentrations could thus be attributed to a wet

deposition event as indeed the weather had been stormy and rainy during the first days of the cruise.

South of 42°N surface concentrations of transect I were uniform in the order of 0.5 nmol L^{-1} Fe until at 39°N the 23°W meridian was reached. During the short north–south transects II to VI between 37°N and 42.5°N along 23°W (see Fig. 1, Fig. 3B and Appendix A), dFe was variable in the range between ∼0.5 and ∼1.5 nmol L^{-1}, possibly reflecting spatio-temporal variability of the dust input (Sedwick et al., 2005; Prospero, 1999) during the period of investigation.

4.2.2. Transects VII–VIII: Northeast Atlantic Ocean

The return transects VII/VIII were begun on March 18 starting at 37°N. Dissolved Fe had become relatively low at about 0.6 nmol L^{-1} and dAl was at 10 nmol L^{-1}. Oceanic dMn remained more or less constant at 0.5 nmol L^{-1} until the continental shelf slope was reached in the Goban Spur area.

4.2.3. Transect VIII: Shelf break and European coastal waters

North of the front at 42.5°N, dFe remained steady at 0.5 nmol L^{-1} until the shelf break. Dissolved Mn and dFe started to increase at 48.78°N, 11.93°W where the water depth was still about 950 m (Fig. 3D), and which was ∼40 km before the continental shelf edge (here defined as the 250 m isobath at 48.84°N, 11.39°W). This short distance off the continental shelf suggests that there is only limited lateral surface transport of dissolved trace metals from the continental shelf into the ocean. This is probably due to the prevailing directions of wind and surface sea currents. Dissolved Fe gradually increased to a concentration of 1.85 nmol L^{-1} at 49.09°N, 9.17°W (∼160 km onto the shelf) followed by a slight decrease to 1.1 nmol L^{-1}. Dissolved Al remained at oceanic values of ∼10 nmol L^{-1} even after crossing the continental margin at a seafloor depth of 140 m until a steep maximum of 56 nmol L^{-1} occurred 450 km after the continental margin, in between the coasts of Brittany (France) and Southwest England, with the seafloor at 75 m depth. This maximum may have been due to a resuspension event. Moran and Moore (1991) suggested that sediment resuspension could be a more important mechanism than diffusion to bring dAl into the overlying water, which in turbulent shallow waters could indeed reach the surface. Dissolved Al remained high in a broad zone with concentrations of 40 nmol L^{-1} during passage through the English Channel, likely as a result of continued sediment resuspension as well as increased atmospheric input and land run-off at this close distance to land masses. Continuing into the Channel, Fe exhibited a sharp increase
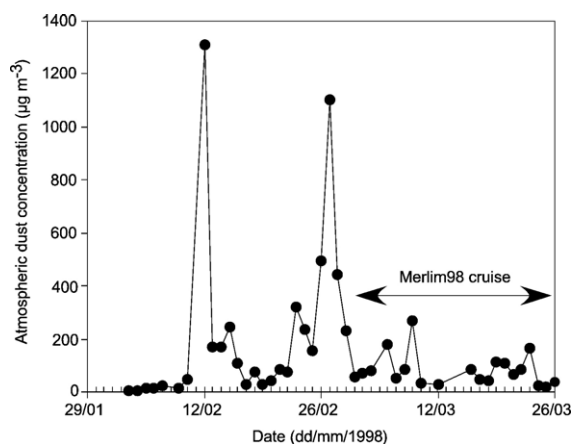
Fig. 6. Dust concentrations measured at the summit of the Pico de la Gorra (1980 m) on the island of Gran Canaria (28°N, 16.5°W). For further details see Torres-Padrón et al. (2002).
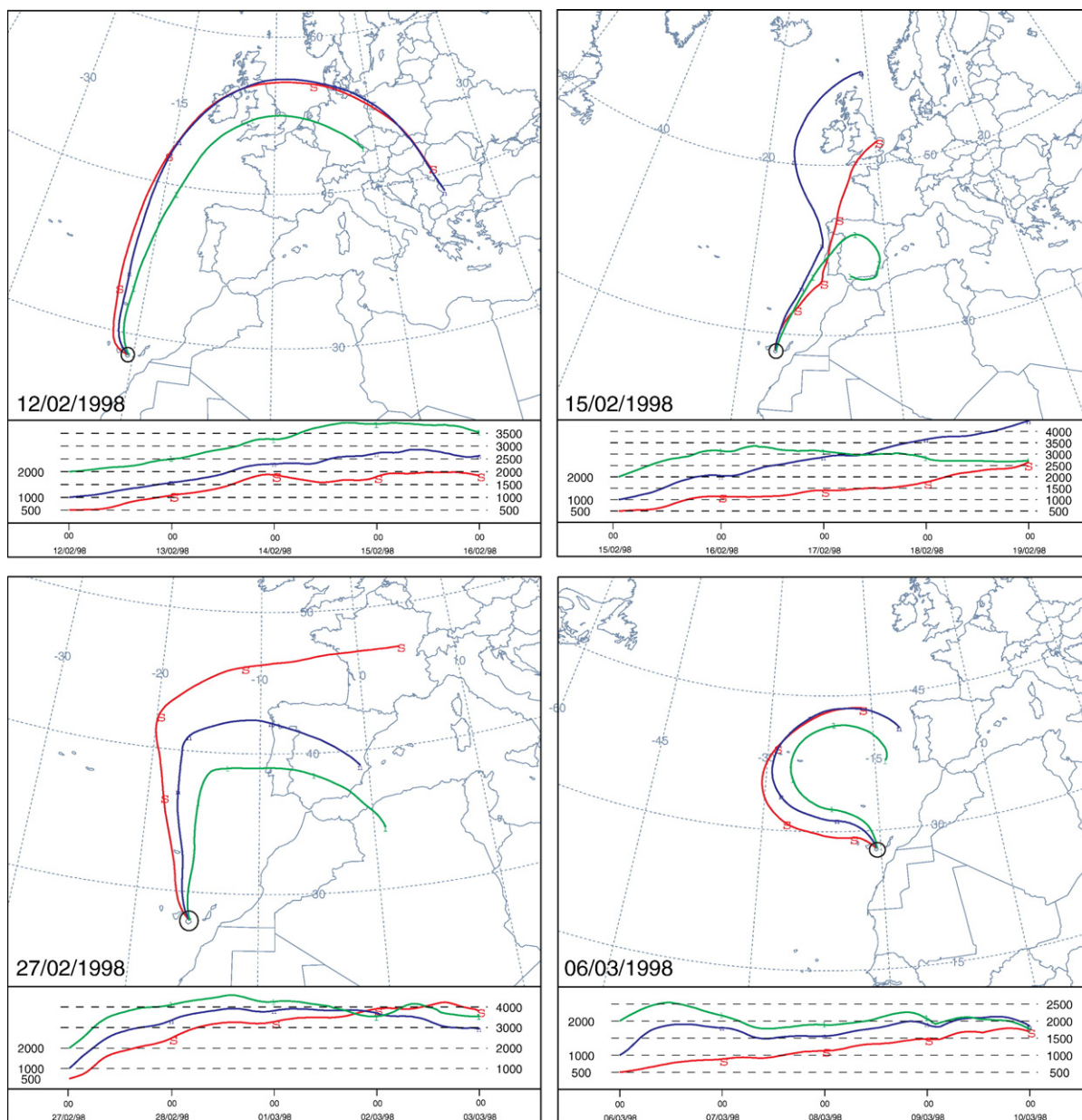
Fig. 7. Ninety-six hour forward air mass trajectories calculated for different altitudes by the NOAA HYSPLIT model, starting point Pico de la Gorra (1980 m) on the island of Gran Canaria (28°N, 16.5°W) on the dates that increased dust concentrations were observed. Label interval: 24 h. CDC Global Reanalysis Grid 1948–2004 used. Red: 500 m altitude, blue: 1000 m altitude, green: 2000 m altitude.

from 1.3 nmol L^{-1} to 4.3 nmol L^{-1} and back again to 2.2 nmol L^{-1} around 50.02°N 01.67°W, together with concomitant maxima of phosphate, nitrate and silicate (Figs. 2C–E and 3D). As also the salinity dropped from 35.60 to 35.35, these observations could possibly be ascribed to the outflow plume or an isolated lens of diluted water from nearby river Seine.

In the Strait of Dover the salinity dropped from 35.4 to 35.0, to go back up to 35.4 in the Southern Bight of the North Sea, indicating fresh water run-off probably from small rivers and streams discharging around the Strait area. Here dFe and dMn were at their highest at 5.9 and 4.9 nmol L^{-1} respectively, with also concomitant increases in nitrate, phosphate and silicate.
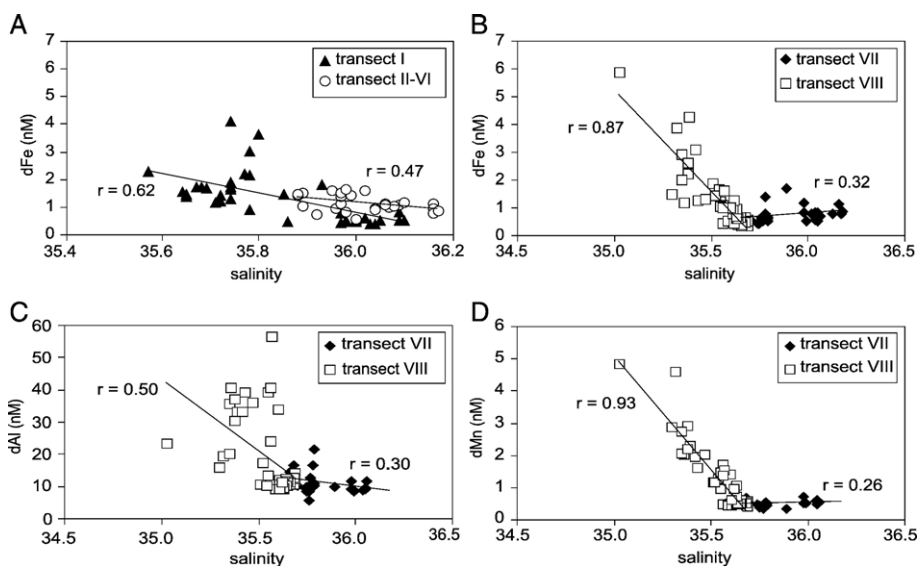
Fig. 8. Dissolved metals versus salinity: A) Fe transects I–VI, B), Fe transects VII–VIII, C) Al transects VII–VIII, D) Mn transects VII–VIII.

4.3. Dissolved aluminium as a proxy of atmospheric dust input

Measures and Vink (2000) and Measures and Brown (1996) used dAl as a proxy for dust deposition in the ocean in a simple model, which was dubbed MADCOW (*Measurement of Aluminium for Dust Calculation in Oceanic Waters*), see below equation 1. This model applies to non-coastal ocean areas and assumes steady state conditions, a global Al residence time τ_{dAl} of 5 yr, a global mixed layer of 30 m, a constant Al content in dust of 8.1% by weight and a solubility of dust derived Al to range between 1.5–5%. We applied the model to our own data with the following modifications: 1) use of solubility estimates for Fe, Mn and Al in Saharan dust, as defined by leaching dust with ammonium acetate at pH 4.7 for 1–2 h (Baker et al., 2006); 2) application of a regionally more relevant average mixed layer depth of 50 m, based on the thermocline depths at stations 8, 9 and 10; 3) use of an upper ocean residence time τ_{dAl} of 4 yr. Orians and Bruland (1986) estimated for the oligotrophic gyre of the North Pacific a τ_{dAl} of 3 to 4 yr. A dAl residence time of 4 yr falls also in the middle of the range as reported for the Sargasso Sea by Jickells (1999) (2.3–6.5 yr) if applied to a 50 m mixed layer.

The variability in the solubility estimates is dominating the uncertainties in the model outcome, so for every calculated estimate the average and the range based on lowest and highest solubility value is given.

One caveat of the MADCOW model is that lateral advection, for instance of Al rich waters towards Al poor waters, was not taken into account. This could lead to overestimation of the dust input in Al poor waters and underestimation in Al rich waters. However, as the open ocean Al gradients during this cruise were low and the sampled water masses generally flowing in the same direction, it is reasonable to assume that horizontal advection was negligible. Another problem is the not fully conservative behavior of Al as it could be biologically scavenged in surface waters, influencing its residence time. As the Chl *a* concentrations were rather low, this probably had no major implications for our research area.

The calculations were made for each surface sample along transects VII and VIII with combined concentration data for Fe, Al and Mn, until ~40 km before the continental rise. Beyond this point the surface metal data suggested other sources than the atmosphere, such as upwelling, sediment and fluvial input.

The dust input D (mg m^{-2} yr^{-1}), was calculated after the equation from Measures et al. (2000, 1996):

$$D = ([dAl]_{sw} M_{Al} z_{mix} / \tau_{dAl}) / (S_{Al} A_{Al}) \qquad (1)$$

where $[dAl]_{sw}$ is the average seawater dAl concentration (μmol m^{-3}), M is atomic weight, z_{mix} the mixed layer depth (50 m), S_{Al} is the Al solubility of Saharan dust from Baker et al. (2006), A_{Al} is the abundance of Al in Saharan dust (6.51 ± 1.58% by weight, Guieu et al., 2002 and references therein), τ_{dAl} is upper ocean residence time of dAl (4 yr).

From the calculated atmospheric dust flux, the atmospheric fluxes of Fe, Mn and Al were calculated:

$$J_{\mathrm{atm,TMe}} = (DA_{\mathrm{Me}})/M_{\mathrm{Me}} \qquad (2)$$

$$J_{\mathrm{atm,dMe}} = S_{\mathrm{Me}}J_{\mathrm{atm,TMe}} \qquad (3)$$

in which $J_{\mathrm{atm,TMe}}$ is the total atmospheric flux (μmol m^{-2} yr^{-1}) of a given metal, $J_{\mathrm{atm,dMe}}$ is dissolved atmospheric flux (μmol m^{-2} yr^{-1}) of a given metal, D is dust input (mg m^{-2} yr^{-1}), A is metal abundance in Saharan dust (Fe: 3.99±0.26%, Guieu et al., 2002; Mn: 0.0712%, Wedepohl, 1995), M_{Me} is atomic weight, and the suffix Me stands for Fe, Mn, or Al respectively. S stands for solubility for which the median values for Saharan dust from Baker et al. (2006) were used. These were: Fe 1.7% (range 1.4–4.1%), Al 3.0% (range 1.9–5.5%) and Mn 55% (range 50–64%).

4.3.1. Steady state atmospheric input

Clear non-steady state conditions such as occurred during transects I–VI are in violation of the model and therefore dust input could not be calculated using the available dAl data from 10 m depths at stations 2 and 6. The steady state dust input to the surface waters was hence calculated for transects VII–VIII only for which we assume that the dAl concentrations have returned to steady state. The average dust input was 1.8 g m^{-2} yr^{-1} (range 1.0–2.9 g m^{-2} yr^{-1}) or 5.0 mg m^{-2} d^{-1} (range 2.8–8.0 mg m^{-2} d^{-1}) (Table 2).

These results are in good agreement with earlier estimates for this ocean region. For instance, they fall near the Northeast Atlantic 1 g m^{-2} yr^{-1} contour line in the global atmospheric deposition model by Duce et al. (1991), which has an uncertainty of a factor 2 to 3. There is a good agreement with the Measures and Brown (1996) results from the IOC1990 cruise with dust input ranging between 0.7–2.4 g m^{-2} yr^{-1} (average 1.6±1.2 g m^{-2} yr^{-1}) at 28°N, ~20°W (the range and standard deviation reflect the Al solubility range of 1.5–5% chosen by Measures and Brown (1996) for their calculation). Recently, Kramer et al. (2004) applied the MADCOW model to their dAl surface data from the

north of Madeira (~33°N, 15°W) and the Canary Basin (30°N, 23°W), directly south from our research area, and obtained here dust inputs ranging from 0.7–0.9 g m^{-2} yr^{-1} and 1.0–2.2 g m^{-2} yr^{-1} respectively.

Transferring the dust input into a dissolved Fe atmospheric flux using an overall Fe solubility of 1.7% (range 1.4–4.1%) from Baker et al. (2006), a dissolved Fe flux of 0.061 μmol m^{-2} d^{-1} (range 0.028–0.23) (Table 2) was obtained, where the range reflects the combined effect of the Fe solubility range and the dust input range.

4.3.2. Estimation of steady state upper ocean residence times of dFe and dMn

Steady state upper ocean residence times were obtained by dividing the inventory of a dissolved metal in the mixed layer by the dissolved atmospheric flux into the mixed layer:

$$\tau_{\mathrm{dMe}} = ([\mathrm{dMe}]_{\mathrm{obs}}z_{\mathrm{mix}})/J_{\mathrm{atm,dMe}} \qquad (4)$$

where τ_{dMe} is the residence times for a dissolved metal, $[\mathrm{dMe}]_{\mathrm{obs}}$ is the measured average dissolved metal concentration at the surface, z_{mix} is the mixed layer depth (50 m), and $J_{\mathrm{atm,dMe}}$ is the dissolved atmospheric flux.

A steady state mean residence times was calculated of 1.3 yr for dFe (range 0.3–2.9 yr), and 1.9 yr for dMn (range 1.0–3.8 yr) at a fixed residence time for dAl of 4 yr.

The dFe residence time found here is longer than previous estimates. De Baar and De Jong (2001) used iron export production and surface ocean iron inventory to obtain a residence time of 0.1–0.3 yr. Several other investigations used directly measured dust fluxes from collected aerosol samples, experimental solubility estimates and upper ocean inventories to arrive at residence times. Jickells (1999) reported residence times in the Western North Atlantic of 0.35 yr for dFe, 4.4 yr for dAl, 5.1 yr for dMn, for a mixed layer of 50 m. Sarthou et al. (2003) found dFe residence times of the order of 0.05–0.08 yr at high dust under the Saharan dust plume. Bergquist and Boyle (2006) calculated for several stations in the North Atlantic surface dFe residence times between 0.1 yr and 0.4 yr. In all likelihood, dFe residence times for the surface ocean would be in the order of a few months,

Table 2
Atmospheric dust and trace metal fluxes from MADCOW model using solubility estimates of Saharan dust (Baker et al., 2006)

	Solubility (%)	Dust flux	Dust flux	Total Al	Total Fe	Total Mn	dAl	dFe	dMn	τ		
	Al, Fe, Mn	mg/m2/d	g/m2/yr	μmol/m2/d	μmol/m2/d	μmol/m2/d	μmol/m2/d	μmol/m2/d	μmol/m2/d	dFe (yrs)	dAl (yrs)	dMn (yrs)
Minimum	5.5, 1.4, 50	2.8	1.0	6.6	2.0	0.036	0.37	0.028	0.018	2.9	4.0	3.8
Maximum	1.9, 4.1, 64	8.0	2.9	19.2	5.7	0.104	0.37	0.234	0.066	0.3	4.0	1.0
Mean	3.0, 1.7, 56	5.0	1.8	12.2	3.6	0.066	0.37	0.061	0.037	1.3	4.0	1.9

consistent with observed seasonal changes and short term variations in iron concentrations (i.e. this work; Sedwick et al., 2005; Boyle et al., 2005). The residence time reported in this work, of somewhat longer than one year, could be attributed to an underestimation of the iron solubility. Baker et al. (2006) found for non-Saharan remote North Atlantic aerosol a median solubility of 7.8%, so if the atmospheric input during this cruise consisted in reality of a mix of Saharan and non-Saharan aerosol, the resulting overall solubility would be in the order of 5%, and the residence time would be shorter by a factor of 3, yielding 0.4 yr. The residence time would also be shorter if we take into account that the observed surface dFe concentrations were not at steady state yet, but still declining and that a steady state surface dFe concentration of ~ 0.35 nmol L^{-1} would be more realistic. If combined, this would finally yield a residence time of about 0.2 yr.

The time it took to return from non-steady state high dFe during transect I to (or close to) steady state during transect VIII while not taking into account any variability in the spatial distribution, could be an expression of the upper ocean response time for the removal of excess dFe and could be estimated at 3–4 weeks or 0.06–0.08 yr.

4.4. Atmospheric Fe input and new production

Dissolved Fe in the ocean usually exhibits nutrient type profiles following nitrate. If we assume that the increase of Fe with depth is due to regeneration of extra- and intracellular Fe associated with sinking biogenic particles, one would expect a relationship with Apparent Oxygen Utilization (AOU) (Bergquist and Boyle, 2006; Sunda, 1997). Indeed, linear correlations between dFe and AOU in the upper 250 m of the NACW at all stations were found (see Table 3). Below 250 m no Fe/ AOU relationship could be established except at station 8. The slope of the regression line gives the $Fe:O_2$ ratio, which is converted into a regenerative Fe:C ratio, by an O_2:C ratio of 1.34 for the Northeast Atlantic (Körtzinger et al., 2001). This O_2:C ratio is lower than the frequently used value of 1.78 by Takahashi et al. (1985) as it takes into account the contribution of anthropogenic CO_2.

It is reasonable to assume that the average regenerative Fe:C ratio of 20 ± 6 μmol Fe:mol C (range 15–30 μmol Fe:mol C) that was thus found (Table 3), would be a representative value for a picophytoplankton dominated phytoplankton community, with the cyanobacterium *Synechococcus* as the numerically dominating species (60–80% of total cell numbers) during this cruise. High values of 120 ± 33 μmol Fe:mol C at the northern station 2 and 81 ± 15 μmol Fe:mol C in the upper 50 m of station 4 (Table 3) were not considered, because these may have been biased by the inferred high dust input at these stations. This possibly influenced the apparent iron requirement by scavenging of extracellular iron onto the cells, or by the storage of luxurious intracellular iron (Blain et al., 2004). Regenerative Fe:C ratios as defined by AOU–dFe relationships may be either overestimated by the presence of preformed dFe, or underestimated due to scavenging of dFe onto particles at greater depth (Bergquist and Boyle, 2006). The NACW present in the upper 900 m is formed between 40°N and 48°N by subduction from the surface layer of the ocean of winter Mode Water and subsequent equatorward transport (Van Aken, 2001). At these

Table 3
Oceanic Fe:C ratios by linear regression of dissolved Fe versus AOU

Station	Location	Depth range (meter)	AOU range (μM)	dFe range (nM)	μmol Fe: mol C [a]	SD [b]	r	n
NACW <250 m								
2 [c]	45°24′N, 10 38′W	25–200	−5.7–2.5	1.13–2.05	120	33	0.88	6
4	40°30′N, 17 47′W	10–50	−15.3–−4.4	0.87–1.53	81	15	0.98	3
4	40°30′N, 17 47′W	75–200	−1.7–25.9	1.07–1.37	16	5	0.90	4
6	37°30′N, 23 00′W	10–250	2.8–45.8	0.83–1.40	17	3	0.95	6
8	42°30′N, 23 00′W	10–250	−6.8–33.5	0.72–1.54	21	6	0.77	10
9	40°00′N, 23 00′W	5–250	−8.7–43.0	0.99–1.77	15	3	0.84	11
10	37°00′N, 23 00′W	5–250	−3.7–45.2	0.52–1.71	30	7	0.92	10
					Average [d]:	20 ± 6		
NACW >250 m								
8	42°30′N, 23°00′W	250–900	33.5–92.1	1.54–1.75	4	2	0.74	4
9	40°00′N, 23°00′W	250–890	43.0–93.8	1.45–1.77	–	–	−0.76	4
10	37°00′N, 23°00′W	250–840	45.2–93.9	1.42–1.88	–	–	0.01	5

[a] Using O_2:C=1.34, Körtzinger et al. (2001).
[b] The error on individual numbers is based on the uncertainty given by the linear regression.
[c] Disregarding dFe 10 m depth (4.53 nM).
[d] Average not taking into account station 2 and station 4 (<50 m).

latitudes east of the Mid-Atlantic Ridge it is unlikely that this water mass receives high preformed dFe. It is usually not under the influence of the Saharan dust plume and situated upwind from Europe, and far enough downwind from the Americas. Also scavenging may have played a limited role because of the relative young age of the water masses considered (Bergquist and Boyle, 2006).

The Fe:C ratios found here with the AOU/dFe relationships are confirmed by the results from a biogeochemical two end member mixing model described by Minster and Boulahdid (1987). This model calculates regenerative Redfield ratios along the linear segment of a salinity—'NO' diagram. 'NO' is a conservative water mass tracer (Broecker, 1974) and is calculated according to: 'NO'$=r_N \times [NO_3] - $ AOU, with r_N being the O_2:N Redfield ratio set at 9 (Körtzinger et al., 2001). End members were chosen at the extremes of the diagram, which should also lie on the geographical borders of the data domain. Redfield ratios were then calculated from the differences between measured and calculated mixing values for the isopycnals 26.95, 27.00, 27.10, 27.20 and 27.40 at the stations 8, 9 and 10, covering a depth range of 88–776 m. Application of this model using O_2:C$=1.34\pm$ 0.06 (Körtzinger et al., 2001) produced the Redfield ratios (Table 4) C:P$=140\pm28$ and N:P$=21\pm4$. For comparison, this is in good agreement with Körtzinger et al. (2001): C:P$=123\pm10$ and N:P$=18\pm2$. The model yielded decreasing regenerative Fe:C ratios with deeper isopycnals (Table 4). In the depth range $\sim100-300$ m the value was 22 ± 5 µmol Fe:mol C and in the depth range below 300 m this was 5 ± 3 µmol Fe:mol C. This agrees well with the results from the dFe/AOU relationships (compare Tables 3 and 4). Apparently the remineralization signal of Fe is higher in the upper water column than lower down,

hinting at preferential remineralization of Fe there. The Fe:C ratios reported here are at the high end of previous reports for the North Atlantic (i.e. 11–17 µmol Fe:mol C, Bergquist and Boyle, 2006; 7–13 µmol Fe:mol C, Sunda, 1997). This may be due still to some luxurious iron in the picophytoplankton. However, values of 20–22 µmol Fe: mol C are in good agreement with previously reported values for bottle experiments with oceanic cyanobacteria. Brand (1991) and Wilhelm and Trick (1995) found respectively 19 and 25 µmol Fe:mol C in iron depleted isolates of *Synechococcus*.

If we take a Fe:C ratio for picophytoplankton of 22 µmol Fe:mol C as the iron requirement, and a mean atmospheric dFe flux into the mixed layer of 0.061 µmol m^{-2} d^{-1}, then an atmospheric iron sustained new production of 33 mg m^{-2} d^{-1} C could be estimated. When compared with integrated Spring primary production in this ocean region of 226 mg m^{-2} d^{-1} C (Teira et al., 2005), this would mean that on average 85% (range 44–93%) of the primary productivity could be supported by regenerated iron.

The inferred high degree of Fe recycling would probably largely take place in the surface mixed layer to be available again, so the required recycling rate of Fe should also be high. It is tentatively postulated that the numerically dominant presence of picophytoplankton could play a pivotal role in keeping relatively high levels of dFe for an extended time period inside the mixed layer by means of 1) iron uptake/adsorption, 2) a low sinking rate, 3) exudation of iron binding siderophores by for instance *Synechococcus* (Hutchins et al., 1999; Wilhelm et al., 1996), in combination with 4) rapid recycling via grazing by zooplankton (Hutchins and Bruland, 1994) and protozoans (Barbeau et al., 1996) as well as release of bioavailable Fe by viral lysis (Poorvin et al., 2004).

Blain et al. (2004) conducted in early Spring 2001 deck incubation experiments at $\sim40°$N, $\sim19°$W at somewhat lower ambient dFe concentrations (~0.4 nmol L^{-1}) as in this work, and found that the larger phytoplankton size class was moderately Fe stressed, and was suffering from co-limitation by the major nutrients N, P and Si as well. The picophytoplankton was responding relatively less strongly to amendments of dFe and/or major nutrients than larger sized phytoplankton, indicating that the former were probably less limited. These findings can be extrapolated to this work, by concluding that at the slightly higher ambient dFe concentrations as were observed here (~0.6 nmol L^{-1}), the dominating picophytoplankton community was likely not Fe limited and perhaps only moderately limited by N and/or P. This is probably related to a higher surface/ volume ratio making the picophytoplankton less diffusion-limited with respect to larger sized cells. Where co-

Table 4
Oceanic Redfield ratios calculated [a] from concentration changes along isopycnal surfaces at stations 8, 9 and 10

Isopycnal	Depth range	Fe/C [b]	C/P	N/P
26.95	88–245	22±6	158±26	24±4
27.00	175–313	23±5	127±51	19±8
27.10	325–463	9±3	153±22	23±3
27.20	513–590	4±1	138±9	20±1
27.40	758–776	2±1	122±7	18±1
	Average	12±9	140±28	21±4
	Literature [c]	7–13, 11–17	123±10	18±2

[a] Two end member mixing model by Minster and Boulahdid (1987). A ratio O_2/C$=1.34$ was used, Körtzinger et al. (2001). O_2/N$=9$ was used to calculate 'NO' as conservative tracer (Broecker, 1974), see text.
[b] µmol Fe:mol C. The error on individual numbers is based on the average of the three stations.
[c] North Atlantic data. Fe/C: Sunda (1997), Bergquist and Boyle (2006). C/P and N/P: Körtzinger et al. (2001).

limitation of Fe, P, N and Si was alleviated, for instance due to deep winter mixing such as could have been the case during transects VII/VIII at 46°N, large phytoplankton will likely start to bloom. At 46°N this could have been a diatom bloom, as Si dropped sharply together with N and P in the Chl *a* maximum (Fig. 2C–F).

4.5. Influence of land run-off on trace metal concentrations on the continental shelf

The Fe, Mn and Al concentrations during the return transect VIII are generally correlated with salinity (Fig. 8B–D) for the samples taken on the continental shelf. The strongest correlation concerns Mn, followed by Fe and then Al. There seems to be mixing on the continental shelf of a low metal/high salinity oceanic end member and a high metal/low salinity coastal end member. Due to the narrow salinity range we can not exclusively attribute the salinity–metal correlation to conservative mixing. Indeed, some scatter in the data for Fe and particularly for Al suggests additional local sources and sinks, such as sediment resuspension, atmospheric inputs and particle readsorption.

The salinity correlation of dMn and dFe would suggest that reductive benthic diffusion did not play a major role at the time of the cruise, as the major spring blooms had not taken place yet. When these blooms decline, the high load of organic matter to the sediment would enhance anaerobic conditions resulting in a diffusive benthic flux of reduced Mn and possibly also Fe (Schoemann et al., 1998). When this benthic flux would have occurred probably a more scattered dissolved metal–salinity relationship would have been found.

5. Conclusions

Surface ocean trace metal data were applied to a simple steady state model to estimate mineral dust flux to the Northeast Atlantic Ocean. Atmospheric dissolved Fe, Mn and Al fluxes were obtained using recent literature values for dust solubility, and upper ocean residence times for these metals were calculated. The atmospheric dust flux results were in good agreement with previously reported data. Upper ocean residence times for steady state conditions were 1.3 yr (range 0.3–2.9 yr) for dFe and 1.9 yr (range 1.0–3.8 yr) for dMn, but may have been overestimated for dFe. A residence time of 0.2–0.4 yr seems to be more realistic. An upper ocean response time for removal of excess dFe under non-steady state conditions of 0.06–0.08 yr was inferred.

Using vertical dFe versus AOU relationships as well as a biogeochemical two end member mixing model, apparent

iron requirements for the *Synechococcus* dominated algal community of respectively 20 ± 6 and 22 ± 5 μmol Fe: mol C were estimated. Combining the latter value with the atmospheric dFe flux, this gave a low estimate of iron supported new production, suggesting that 85% of primary productivity could be sustained by regenerated dFe in the surface mixed layer. It is suggested that picophytoplankton plays a pivotal role in this, by exudation of iron binding siderophores and low sinking velocities, in combination with protozoan and zooplankton grazing as well as viral lysis. Ambient dFe concentrations during this cruise were probably not limiting picophytoplankton but larger phytoplankton was likely co-limited by dFe and major nutrients, notions supported by incubation work by Blain et al. (2004). Enhanced surface trace metal concentrations were observed at the beginning of the cruise, probably related to an episode of enhanced Saharan dust input over the Northeast Atlantic Ocean prior and during the period of investigation. The local and episodic nature of these enhanced dust fluxes, in combination with occurring co-limitation of the major nutrients, makes that their influence on overall primary productivity and phytoplankton community structure is probably minimal in the investigated ocean area. Only when co-limitation factors are alleviated can a dust input event have effect on the ecosystem.

More or less strong dissolved metal–salinity relationships on the continental shelf hint at a probably mostly fluvial source for dFe and dMn but likely a sediment resuspension or atmospheric origin for dAl. The continental shelf is probably not a major source of trace metals to the surface of the adjacent open ocean.

Appendix A. Transect data

Transect	Date	Time (UT)	Lat (dec)	Long (dec)	Sal	Temp	dFe (nM)	dMn (nM)	dAl (nM)	Si (µM)	PO$_4$ (µM)	NO$_3$ (µM)
I	3/6/1998	13:00	47.33	−7.53	35.57		2.28			2.39	0.40	6.47
Shelf	3/6/1998	15:00	47.23	−7.72	35.65	12.02	1.47			2.35	0.39	6.28
Break	3/6/1998	16:00	47.18	−7.82	35.64		1.56			2.31	0.38	6.09
	3/6/1998	17:00	47.10	−7.94	35.65		1.39			2.20	0.36	5.80
	3/6/1998	18:00	47.03	−8.05	35.72	12.43	1.43			2.08	0.34	5.60
	3/6/1998	19:00	46.95	−8.17	35.69	12.25	1.69			2.00	0.33	5.32
	3/6/1998	21:00	46.78	−8.42	35.68	12.24	1.72			2.03	0.32	5.39
	3/7/1998	0:00	46.53	−8.81	35.67	12.10	1.72			2.49	0.32	5.34
	3/7/1998	4:00	46.23	−9.30	35.72	12.39	1.20			2.00	0.33	5.29
	3/7/1998	8:00	45.88	−9.87	35.71	12.48	1.18			1.78	0.29	4.67
	3/7/1998	9:00	45.77	−10.02	35.72	12.58	1.41			1.71	0.25	4.29
	3/7/1998	10:00	45.67	−10.17	35.74	12.69	1.28			1.80	0.27	4.50
	3/7/1998	11:00	45.60	−10.28	35.74	12.79	1.62			1.90	0.29	4.83
	3/7/1998	12:00	45.52	−10.42	35.74	12.55	1.72			1.96	0.32	4.97
	3/7/1998	13:00	45.41	−10.59	35.74	12.55	1.63			2.00	0.33	4.97
	3/7/1998	17:00	45.16	−10.99	35.74	13.10	1.88			1.61	0.22	3.53
	3/7/1998	20:00	44.80	−11.52	35.74	13.10	4.09			1.60	0.21	3.39
	3/8/1998	0:00	44.38	−12.15	35.77	13.14	2.22			1.51	0.22	3.49
	3/8/1998	4:00	44.02	−12.68	35.78	13.38	2.15			1.46	0.20	3.12
	3/8/1998	9:00	43.52	−13.46	35.78	13.24	3.02			1.35	0.17	2.52
	3/8/1998	12:00	43.23	−13.91	35.80	13.60	3.62			1.34	0.15	2.18
	3/8/1998	15:00	43.01	−14.24	35.78	13.72	0.90			1.24	0.13	1.90
	3/8/1998	17:00	42.75	−14.61	35.93	14.32	1.80			1.13	0.08	0.84
	3/8/1998	19:00	42.52	−14.93	35.85	14.00	1.48			1.16	0.11	1.10
	3/9/1998	0:00	41.95	−15.83	35.86	14.02	0.48			1.32	0.12	1.10
	3/9/1998	10:00	40.72	−17.56	35.97	15.12	0.43			1.18	0.01	0.18
	3/9/1998	11:00	40.60	−17.73	36.00	15.11	0.58			1.18	0.02	0.15
	3/9/1998	15:00	40.50	−17.86	35.98	15.17	0.52			1.17	0.03	0.01
	3/9/1998	17:00	40.27	−18.19	36.00	15.38	0.48			1.20	0.04	0.00
	3/9/1998	20:00	39.89	−18.74	36.02	15.42	0.63			1.15	0.01	0.00
	3/10/1998	0:00	39.64	−19.56	35.97	15.12	0.77			1.30	0.03	0.47
	3/10/1998	4:00	39.46	−20.47	35.98	15.17	0.49			1.30	0.01	0.37
	3/10/1998	8:00	39.30	−21.38	36.09	15.78	0.54			0.98	0.01	0.00
	3/10/1998	10:00	39.21	−21.85	36.04	15.75	0.38			1.05	0.00	0.00
	3/10/1998	12:00	39.15	−22.22	36.03	15.68	0.38			1.04	0.01	0.00
	3/10/1998	15:00	39.08	−22.53	36.05	15.84	0.52			1.02	0.01	0.02
	3/10/1998	17:00	39.03	−22.79	36.10	16.31	0.50			1.00	0.01	0.04
	3/10/1998	20:00	38.87	−23.01	36.09	16.14	0.84			0.96	0.01	0.00
II	3/11/1998	0:00	38.48	−22.99	36.16	16.31	1.12			0.95	0.01	0.00
	3/11/1998	20:00	37.85	−23.00	36.09	16.09	1.07			1.04	0.01	0.00
III	3/12/1998	0:00	38.33	−22.99	36.10	16.02	1.17			0.96	0.01	0.00
	3/12/1998	4:00	38.88	−23.00	36.07	15.74	0.99			0.98	0.01	0.00
	3/12/1998	8:00	39.40	−23.00	36.04	15.72	0.96			1.01	0.02	0.00
	3/12/1998	10:00	39.68	−23.00	36.06	15.58	1.13			1.06	0.02	0.13
	3/12/1998	12:00	39.89	−23.00	36.00	15.43	0.57			1.05	0.02	0.06
IV	3/12/1998	16:00	40.30	−22.98	35.96	15.30	0.93			1.22	0.03	0.70
	3/12/1998	18:00	40.26	−23.00	35.98	15.08	0.81			1.36	0.05	1.23
	3/13/1998	0:00	41.17	−23.00	35.92	14.56	0.74			1.17	0.02	0.21
	3/13/1998	4:00	41.88	−22.99	35.97	14.86	1.13			1.35	0.05	1.28
	3/13/1998	8:00	42.58	−23.00	35.89	14.10	1.05					
V	3/15/1998	16:00	42.52	−23.03	35.89	14.20	1.50			1.69	0.14	2.93
	3/15/1998	17:00	42.37	−23.00	35.88	14.28	1.42			1.63	0.10	2.31
	3/15/1998	18:00	42.22	−23.00	35.88	14.24	1.49			1.70	0.12	2.56
	3/15/1998	20:00	41.93	−23.00	35.97	14.86	1.38			1.27	0.02	0.69
	3/15/1998	22:00	41.62	−22.99	35.99	15.09	1.42			1.22	0.03	0.72
	3/16/1998	0:00	41.27	−23.02	35.95	14.92	1.60			1.13	0.02	0.55
	3/16/1998	2:00	40.94	−22.99	35.97	14.94	1.50			1.24	0.07	1.69

Appendix A (*continued*)

Transect	Date	Time (UT)	Lat (dec)	Long (dec)	Sal	Temp	dFe (nM)	dMn (nM)	dAl (nM)	Si (µM)	PO$_4$ (µM)	NO$_3$ (µM)
	3/16/1998	4:00	40.61	−22.99	35.98	15.04	1.64			1.36	0.05	0.95
	3/16/1998	6:00	40.27	−22.99	36.02	15.46	1.61			1.14	0.02	0.16
VI	3/17/1998	16:00	39.92	−23.00	36.08	16.02	1.05			1.01	0.03	0.09
	3/17/1998	18:00	39.55	−22.97	36.06	15.64	1.08			1.00	0.03	0.12
	3/17/1998	20:00	39.18	−22.99	36.04	15.74	0.89			1.01	0.03	0.05
	3/17/1998	22:00	38.81	−23.00	36.16	16.16	0.95			1.01	0.02	0.03
	3/18/1998	0:00	38.44	−22.99	36.16	16.16	0.78			0.91	0.02	0.02
	3/18/1998	2:00	38.07	−23.01	36.17	16.20	0.86			0.92	0.02	0.02
	3/18/1998	4:00	37.70	−23.01	36.16	16.08	0.78			0.93	0.01	0.02
	3/18/1998	6:00	37.34	−23.00	36.17	16.44	0.87			0.95	0.02	0.03
VII	3/19/1998	21:00	37.14	−23.00	36.16	16.56	1.12			0.94	0.01	003
	3/20/1998	0:00	37.67	−23.01	36.18	16.33	0.87			1.04	0.02	0.00
	3/20/1998	2:00	38.02	−23.02	36.17	16.24	0.78			1.00	0.02	0.00
	3/20/1998	4:00	38.37	−23.01	36.13	16.04	0.78			1.00	0.01	0.01
	3/20/1998	6:00	38.72	−23.00	36.02	15.54	0.78			1.03	0.01	0.00
	3/20/1998	8:00	39.06	−23.00	36.04	15.54	0.84			1.10	0.02	0.00
	3/20/1998	10:00	39.41	−23.00	36.05	15.56	0.54	0.49	9.09	1.07	0.02	0.00
	3/20/1998	12:00	39.74	−22.99	36.05	15.67	0.81	0.62	9.49	1.08	0.01	0.00
	3/20/1998	14:00	40.07	−23.00	36.06	15.73	0.68	0.54	11.64	1.07	0.01	0.01
	3/20/1998	16:00	40.41	−23.00	36.04	15.59	0.55	0.58	8.95	1.04	0.01	0.02
	3/20/1998	18:00	40.75	−23.01	35.98	15.39	1.17	0.71	11.57	1.08	0.01	0.01
	3/20/1998	20:00	41.09	−23.00	35.98	15.00	0.82	0.50	9.26	1.16	0.03	0.81
	3/20/1998	22:00	41.43	−23.00	35.99	15.11	0.51	0.50	8.51	1.29	0.05	0.43
	3/21/1998	0:00	41.75	−23.01	35.99	15.11	0.50	0.52	8.71	1.19	0.04	0.16
	3/21/1998	2:00	42.07	−23.01	35.89	14.28	(1.69)	0.36	9.94	1.37	0.04	0.53
	3/21/1998	4:00	42.38	−23.00	35.79	13.78	0.53	0.52	(21.65)	1.67	0.13	2.28
	3/21/1998	6:00	42.57	−23.00	35.78	13.76	0.79	0.54	(16.75)	2.11	0.20	3.39
	3/21/1998	8:00	42.60	−23.00	35.78	13.66	(1.39)	0.44	9.94	2.09	0.21	3.42
	3/21/1998	10:00	42.76	−22.99	35.76	13.65	0.64	0.42	5.65	1.25	0.15	1.97
	3/21/1998	12:00	43.11	−23.01	35.76	13.74	0.59	0.40	8.44	1.69	0.14	2.09
	3/21/1998	14:00	43.47	−23.01	35.79	13.60	0.63	0.43	10.35	1.97	0.23	3.48
	3/21/1998	16:00	43.82	−23.01	35.77	13.40	0.54	0.39	10.62	2.51	0.27	4.31
	3/21/1998	18:00	44.17	−22.99	35.79	13.64	0.64	0.50	11.03	2.48	0.30	5.11
	3/21/1998	20:00	44.52	−22.99	35.77	13.48	0.69	0.36	12.53	2.49	0.31	5.06
	3/21/1998	22:00	44.87	−22.99	35.70	12.94	0.54	0.50	10.18	2.98	0.37	6.05
	3/22/1998	0:00	45.23	−23.02	35.74	13.04	0.42	0.47	9.57	3.70	0.49	7.86
	3/22/1998	2:00	45.59	−23.01	35.75	13.08	0.44	0.45	9.94	2.58	0.33	5.07
	3/22/1998	4:00	45.96	−23.00	35.75	13.06	0.47	0.39	8.31	2.29	0.30	4.27
	3/22/1998	6:00	46.32	−22.99	35.69	12.78	0.54	0.47	n.a.	2.57	0.33	5.18
	3/22/1998	8:00	46.67	−23.00	35.66	12.57	0.47	0.63	14.50	3.23	0.46	7.30
	3/22/1998	10:00	47.02	−23.01	35.68	12.88	0.65	0.68	16.61	3.20	0.44	7.18
VIII	3/22/1998	12:00	47.37	−22.99	35.69	12.85	0.56	0.58	14.27	3.29	0.45	7.17
	3/22/1998	14:00	47.54	−22.69	35.69	12.72	0.35	0.55	11.57	3.28	0.43	7.18
	3/22/1998	16:00	47.59	−22.20	35.61	12.24	0.49	0.54	12.12	3.34	0.44	7.33
	3/22/1998	18:00	47.65	−21.70	35.60	12.20	0.54	0.51	9.74	3.30	0.44	7.24
	3/22/1998	20:00	47.69	−21.00	35.63	12.26	0.45	0.49	10.69	3.38	0.47	7.55
	3/22/1998	22:00	47.75	−20.73	35.56	11.74	0.45	0.49	10.55	3.34	0.46	7.37
	3/23/1998	0:00	47.82	−20.23	35.59	11.97	0.52	0.45	9.05	3.32	0.51	8.16
	3/23/1998	2:00	47.90	−19.74	35.63	12.27	0.76	0.49	11.16	3.30	0.47	7.62
	3/23/1998	4:00	47.97	−19.23	35.68	12.28	0.67	0.46	10.48	2.98	0.43	7.05
	3/23/1998	6:00	48.02	−18.73	35.69	12.37	0.51	0.42	12.36	3.10	0.43	7.19
	3/23/1998	8:00	48.06	−18.21	35.68	12.32	0.50	0.51	12.56	3.01	0.45	7.19
	3/23/1998	10:00	48.12	−17.69	35.64	12.20	0.39	0.52	12.48	3.17	0.47	7.49
	3/23/1998	12:00	48.18	−17.17	35.65	12.14	0.50	0.49	10.25	3.00	0.45	7.44
	3/23/1998	14:00	48.23	−16.66	35.66	12.14	0.34	0.50	10.74	3.06	0.47	7.56
	3/23/1998	16:00	48.30	−16.15	35.66	12.10	0.41	0.63	11.35	3.26	0.51	8.18
	3/23/1998	18:00	48.36	−15.63	35.62	11.91	0.42	0.50	10.66	2.99	0.47	7.59
	3/23/1998	20:00	48.41	−15.09	35.65	11.97	0.64	0.50	11.55	3.15	0.48	7.66
	3/23/1998	22:00	48.48	−14.56	35.63	11.65	0.62	0.50	10.65	3.15	0.49	7.91

Appendix A (*continued*)

Transect	Date	Time (UT)	Lat (dec)	Long (dec)	Sal	Temp	dFe (nM)	dMn (nM)	dAl (nM)	Si (μM)	PO$_4$ (μM)	NO$_3$ (μM)
	3/24/1998	0:00	48.55	−14.03	35.61	11.53	0.80	0.44	10.74	2.57	0.39	5.63
	3/24/1998	2:00	48.61	−13.51	35.63	11.80	0.59	0.49	10.05	3.29	0.54	8.52
	3/24/1998	4:00	48.65	−12.99	35.63	11.69	0.67	0.58	10.86	3.45	0.54	8.54
	3/24/1998	6:00	48.72	−12.47	35.64	11.68	0.62	0.52	10.13	3.29	0.51	8.21
Shelf	3/24/1998	8:00	48.78	−11.93	35.63	11.67	0.69	0.72	9.32	2.86	0.46	7.48
Break	3/24/1998	10:00	48.84	−11.39	35.63	11.66	0.95	1.06	9.64	2.94	0.47	7.59
	3/24/1998	12:00	48.90	−10.84	35.61	11.52	0.96	0.63	9.32	3.00	0.45	7.18
	3/24/1998	14:00	48.97	−10.29	35.62	11.56	1.27	0.95	11.47	2.87	0.44	6.77
	3/24/1998	18:00	49.09	−9.17	35.51	10.94	1.85	1.18	10.45	2.51	0.40	5.93
	3/24/1998	20:00	49.13	−8.64	35.54	11.08	1.64	1.28	10.25	2.34	0.37	5.81
	3/24/1998	22:00	49.22	−8.10	35.55	10.94	1.23	0.95	13.49	2.35	0.38	5.64
	3/25/1998	0:00	49.28	−7.52	35.52	10.84	1.42	1.15	17.22	2.57	0.39	5.63
	3/25/1998	2:00	49.34	−6.93	35.56	10.90	1.07	1.70	23.83	2.10	0.35	4.91
	3/25/1998	4:00	49.41	−6.34	35.60	10.96	1.01	1.41	33.83	2.24	0.30	4.28
	3/25/1998	6:00	49.47	−5.78	35.55	10.82	1.06	1.46	39.10	2.33	0.23	3.53
	3/25/1998	8:00	49.53	−5.25	35.57	10.74	1.60	1.55	56.33	2.52	0.19	3.47
	3/25/1998	10:00	49.60	−4.74	35.56	10.68	1.01	1.36	40.75	2.44	0.26	4.40
	3/25/1998	12:00	49.65	−4.19	35.43	10.10	1.28	1.62	39.27	2.58	0.28	4.82
	3/25/1998	14:00	49.71	−3.61	35.36	9.82	1.16	2.03	40.75	3.10	0.35	7.39
	3/25/1998	16:00	49.78	−2.99	35.47	9.94	1.29	2.01	36.04	2.62	0.32	6.25
	3/25/1998	18:00	49.90	−2.34	35.35	9.70	2.91	2.05	35.57	1.90	0.35	6.13
	3/25/1998	20:00	50.02	−1.67	35.39	9.70	4.26	2.29	33.01	2.00	0.39	7.16
	3/25/1998	22:00	50.13	−1.10	35.42	9.64	3.07	1.95	33.34	2.07	0.37	7.06
	3/26/1998	0:00	50.21	−0.64	35.38	9.50	2.20	2.21	30.31	2.05	0.35	6.92
	3/26/1998	2:00	50.28	−0.19	35.38	9.42	2.60	2.92	37.05	1.48	0.27	5.65
	3/26/1998	4:00	50.37	0.32	35.30	9.18	1.46	2.88	16.03	0.74	0.17	3.93
	3/26/1998	6:00	50.46	0.89	35.32	8.91	3.87	4.58	19.53	0.71	0.08	1.12
	3/26/1998	10:00	51.09	1.68	35.03	8.59	5.87	4.85	23.44	2.34	0.28	7.14
	3/26/1998	12:00	51.40	2.08	35.35	8.81	2.00	2.74	20.07	2.34	0.28	7.14

Appendix B. Station data

Date	Station	Position	Depth (m)	Sal	Temp	dFe (nM)	dMn (nM)	dAl (nM)	Si (μM)	PO$_4$ (μM)	NO$_3$ (μM)	AOU (μM)
3/7/1998	2	45°24′N	10	35.71	12.42	4.53	3.13	40.46	1.91	0.40	5.52	−4.8
		10°38′W	25	35.71	12.41	1.13	2.11	30.79	1.92	0.42	5.53	−5.7
			50	35.71	12.42	1.34	0.79	13.04	2.08	0.39	5.53	−4.8
			75	35.71	12.40	1.50	1.49	18.56	1.94	0.38	5.53	−5.2
			125	35.71	12.40	1.74	1.23	26.68	1.96	0.36	5.60	−4.7
			150	35.70	12.09	1.99	0.98	22.73	1.98	0.42	6.32	0.8
			200	35.66	12.04	2.05	1.50	20.21	2.00	0.49	7.86	2.5
3/9/1998	4	40°30′N	10	36.01	15.20	0.87	0.42	9.50	1.24	0.00	0.20	−15.3
		17°48′W	30	36.01	15.03	1.30	1.16	15.45	1.19	0.01	0.52	−10.0
			50	36.01	14.99	1.53	1.08	10.45	1.21	0.03	0.90	−4.4
			75	36.00	14.97	1.07	0.46	13.95	1.24	0.09	1.15	−1.7
			125	35.95	14.58	0.99	(1.02)	14.93	1.41	0.18	2.19	1.5
			150	35.95	14.48	1.10	0.33	15.76	2.18	0.41	6.35	13.6
			200	35.83	13.17	1.37	0.19	17.43	3.28	0.61	9.32	25.9
3/11/1998	6	37°29′N	10	36.13	16.43	0.83	0.65	21.37	1.01	0.01	0.04	2.8
		22°59′W	30	36.13	16.35	0.88	0.81	(41.73)	1.07	0.03	0.01	1.9
			50	36.13	16.21	0.93	0.49	11.36	1.04	0.03	0.03	3.8
			75	36.15	16.09	1.00	0.94	21.93	1.02	0.06	0.21	10.1
			100	36.15	15.93	1.18	0.57	17.45	1.04	0.07	0.48	14.8
			250	35.83	13.21	1.40	0.09	17.51	3.21	0.58	9.44	45.8
			1000	35.69	9.13	1.31	0.07	30.32	9.75	1.10	17.85	95.5
			1500	35.23	5.08	1.30	0.11	24.34	10.32	1.04	16.83	66.5

Appendix B (*continued*)

Date	Station	Position	Depth (m)	Sal	Temp	dFe (nM)	dMn (nM)	dAl (nM)	Si (μM)	PO₄ (μM)	NO₃ (μM)	AOU (μM)
			2000	35.00	3.73	1.78	0.09	16.45	12.79	1.18	18.32	63.5
3/13/1998	8	42°36′N	10	35.80	13.75	0.83	0.49	13.15	1.89	0.22	3.53	−6.8
		23°00′W	20	35.78	13.64	0.74	0.40	14.32	1.89	0.22	3.31	−9.1
			30	35.80	13.63	0.72	0.44	12.14	1.90	0.22	3.32	−7.5
			40	35.79	13.57	1.16	0.49	n.a.	1.88	0.24	3.66	−5.5
			50	35.78	13.55	1.22	0.50	12.08	1.81	0.27	3.79	−2.8
			75	35.75	13.32	1.23	0.49	12.42	1.84	0.28	3.96	−2.7
			100	35.75	13.26	1.05	0.67	10.80	1.89	0.29	4.04	−3.2
			150	35.75	13.13	1.13	0.53	12.98	2.18	0.36	5.60	3.3
			200	35.75	12.99	1.12	0.37	n.a.	2.64	0.44	7.08	9.4
			250	35.67	12.37	1.54	0.30	14.32	3.71	0.63	10.32	33.5
			500	35.51	10.92	1.49	0.36	15.11	4.97	0.80	13.15	52.7
			750	35.45	9.00	1.60	0.18	17.40	9.05	1.14	18.19	91.6
			900	35.34	8.78	1.75	0.18	22.04	10.32	1.18	18.83	92.1
			1000	35.46	7.43	1.72	0.14	20.70	10.80	1.19	19.05	86.1
			1500	34.99	4.22	1.86	0.18	15.78	10.00	1.14	18.06	51.0
			1750	34.93	3.72	1.96	0.20	14.38	11.14	1.17	18.08	39.8
			2000	34.90	3.45	1.97	0.19	13.48	12.17	1.18	18.05	32.2
3/16/1998	9	40°00′N	5	36.06	15.76	1.26	0.72	14.54	1.03	0.00	0.10	−8.7
		23°00′W	15	36.06	15.65	1.13	0.53	17.43	1.06	0.00	0.11	−7.4
			20	36.06	15.63	1.03	0.78	12.80	1.06	0.00	0.09	−7.8
			30	36.06	15.59	0.99	0.63	14.01	1.05	0.00	0.09	−8.7
			40	36.06	15.59	1.29	0.54	16.96	1.10	0.01	0.21	−7.7
			50	36.04	15.56	1.35	0.53	11.50	1.12	0.01	0.24	−8.3
			65	36.03	15.36	1.38	0.54	(15.79)	1.20	0.08	1.71	6.7
			115	35.96	14.76	1.35	0.50	11.86	1.68	0.21	3.85	3.7
			165	35.92	14.53	1.41	0.47	14.41	1.79	0.24	4.30	5.9
			200	35.90	14.36	1.30	0.45	n.a.	1.73	0.20	3.57	14.8
			250	35.81	13.52	1.77	0.34	15.86	3.08	0.48	8.66	43.0
			500	35.51	11.38	1.65	0.18	14.54	5.74	0.75	13.67	61.8
			700	35.44	10.04	1.45	0.19	16.20	8.26	1.04	17.33	84.7
			890	35.67	9.79	1.61	0.17	24.00	9.87	1.09	18.05	93.8
			1000	35.62	9.12	1.54	0.16	23.68	10.36	1.09	18.03	91.8
			1065	35.69	9.00	1.60	0.22	23.85	10.45	1.10	17.32	90.3
			1250	35.34	6.62	1.76	0.24	19.15	11.51	1.16	18.71	73.9
			1500	35.03	4.76	1.80	0.25	15.46	11.62	1.16	18.41	55.2
			2000	34.95	3.72	1.71	0.36	14.95	13.44	1.15	18.11	36.2
3/18/1998	10	37°00′N	10	36.11	16.48	0.73	1.08	12.72	0.95	0.02	0.06	−3.7
		23°00′W	20	36.11	16.44	0.66	0.90	12.74	0.95	0.00	0.11	−1.8
			30	36.11	16.43	0.52	0.88	9.36	0.91	0.01	0.04	−1.9
			40	36.11	16.42	0.79	1.08	12.17	0.93	0.01	0.04	−0.9
			50	36.11	16.42	0.70	0.89	11.00	0.90	0.04	0.34	−1.6
			75	36.08	15.96	0.95	0.87	n.a.	1.02	0.07	1.52	8.4
			100	36.03	15.64	0.92	0.82	10.29	1.18	0.10	2.11	9.1
			125	35.99	15.37	1.47	0.72	10.07	1.28	0.11	2.69	13.8
			150	35.98	15.05	1.23	0.43	13.55	2.31	0.34	6.37	23.9
			200	35.87	13.78	1.51	0.35	15.49	3.35	0.52	9.22	35.9
			250	35.81	13.44	1.71	0.29	n.a.	3.53	0.56	9.70	45.2
			500	35.56	11.41	1.42	0.19	19.45	5.86	0.86	14.37	65.9
			650	35.45	10.24	1.67	0.21	20.23	8.14	1.05	17.67	82.8
			770	35.57	10.10	1.37	0.16	22.45	9.04	1.06	17.68	92.1
			840	35.57	9.64	1.88	0.18	24.34	9.95	1.12	18.26	93.9
			960	35.61	8.90	1.59	0.17	26.29	10.51	1.12	18.12	91.9
			1250	35.43	6.91	1.44	0.20	21.73	11.43	1.14	18.40	75.3
			1500	35.23	5.41	1.64	0.30	18.32	11.94	1.15	18.25	62.9
			2000	35.05	3.95	1.73	0.18	18.79	16.10	1.21	18.66	47.3

References

Barbeau, K., Moffet, J.W., Caron, M.A., Croot, P.L., Erdner, D.L., 1996. Role of protozoan grazing in relieving iron limitation of phytoplankton. Nature 380, 61–64.

Baker, A.R., Jickells, T.D., Witt, M., Linge, K.L., 2006. Trends in the solubility of iron, aluminium, manganese and phosphorus in aerosol collected over the Atlantic Ocean. Marine Chemistry 98, 43–58.

Bergquist, B.A., Boyle, E.A., 2006. Dissolved iron in the tropical and subtropical Atlantic Ocean. Global Biogeochemical Cycles 20, GB1015. doi:10.1029/2005GB002505.

Blain, S., Guieu, C., Claustre, H., Leblanc, K., Moutin, T., Quéquiner, B., Ras, J., Sarthou, G., 2004. Availability of iron and major nutrients for phytoplankton in the northeast Atlantic Ocean. Limnology and Oceanography 49, 2095–2104.

Bowie, A.R., Withworth, D.J., Achterberg, E.P., Mantoura, R.F.C., Worsfold, P.J., 2002. Biogeochemistry of Fe and other trace elements (Al, Co, Ni) in the upper Atlantic Ocean. Deep-sea Research. Part 1. Oceanographic Research Papers 49, 605–636.

Bowie, A.R., Achterberg, E.P., Croot, P.L., de Baar, H.J.W., Laan, P., Moffett, J.W., Ussher, S., Worsfold, P.J., 2006. A community-wide intercomparison exercise for the determination of dissolved iron in seawater. Marine Chemistry 98, 81–99.

Boyd, P.W., et al., 2000. Phytoplankton bloom upon mesoscale iron fertilisation of polar Southern Ocean waters. Nature 407, 695–702.

Boyé, M., Aldrich, A.P., Van den Berg, C.M.G., De Jong, J.T.M., Veldhuis, M., De Baar, H.J.W., 2003. Horizontal gradient of the chemical speciation of iron in surface waters of the Northeast Atlantic Ocean. Marine Chemistry 80, 129–143.

Boyle, E.A., Bergquist, B.A., Kayser, R.A., Mahowald, N., 2005. Iron, manganese and lead at Hawaii Ocean Time-series ALOHA: temporal variability and an intermediate water hydrothermal plume. Geochimica et Cosmochimica Acta 69, 933–952.

Boyé, M., Aldrich, A.P., Van den Berg, C.M.G., De Jong, J.T.M., Nirmaier, H., Veldhuis, M., Timmermans, K.R., De Baar, H.J.W., 2006. The chemical speciation of iron in the Northeast Atlantic Ocean. Deep-sea Research. Part 1. Oceanographic Research Papers 53, 667–683.

Brand, L.E., 1991. Minimum iron requirements of marine phytoplankton and the implications for the biogeochemical control of new production. Limnology and Oceanography 36, 1756–1771.

Broecker, W.S., 1974. 'NO', a conservative water-mass tracer. Earth and Planetary Science Letters 23, 100–107.

Coale, K.H., et al., 1996. A massive phytoplankton bloom induced by an ecosystem-scale iron fertilisation experiment in the equatorial Pacific Ocean. Nature 383, 495–501.

De Baar, H.J.W., De Jong, J.T.M., 2001. Distributions, Sources and Sinks of Iron in Seawater. In: Turner, D., Hunter, K. (Eds.), The Biogeochemistry of Iron in Seawater, IUPAC Book Series on Analytical and Physical Chemistry of Environmental Systems, vol. 7. John Wiley & Sons Ltd, Chichester, pp. 123–253.

De Jong, J.T.M., Den Das, J., Bathmann, U., Stoll, M.H.C., Kattner, G., Nolting, R.F., De Baar, H.J.W., 1998. Dissolved iron at subnanomolar levels in the Southern Ocean as determined by shipboard analysis. Analytica Chimica Acta 377, 114–124.

De Jong, J.T.M., Boyé, M., Schoemann, V.F., Nolting, R.F., De Baar, H.J.W., 2000. Shipboard techniques based on flow injection analysis for measuring dissolved Fe, Mn and Al in seawater. Journal of Environmental Monitoring 2, 496–502.

Draxler, R.R., Rolph, G.D., 2001. HYSPLIT (HYbrid Single-Particle Lagrangian Integrated Trajectory) Model access via NOAA ARL READY Website. NOAA Air Resources Laboratory, Silver Spring, MD, USA (http://www.arl.noaa.gov/ready/hysplit4.html).

Duce, R.A., Tindale, N.W., 1991. Atmospheric transport of iron and its deposition in the ocean. Limnology and Oceanography 36, 1715–1726.

Duce, R.A., et al., 1991. The atmospheric input of trace species to the world ocean. Global Biogeochemical Cycles 5, 193–259.

Gehlen, M., Beck, L., Calas, G., Flank, A.-M., Van Bennekom, A.J., Van Beusekom, J.E.E., 2002. Unraveling the atomic structure of biogenic silica: evidence of the structural association of Al and Si in diatom frustules. Geochimica et Cosmochimica Acta 66, 1601–1609.

Grasshoff, K., Ehrhardt, M., Kremling, K., 1983. Methods of Seawater Analysis. Verlag Chemie, Weinheim, Germany.

Guieu, C., Loÿe-Pilot, M.-D., Ridame, C., Thomas, C., 2002. Chemical characterization of the Saharan dust end-member: some biogeochemical implications for the western Mediterranean Sea. Journal of Geophysical Research 107 (D15). doi:10.1029/2001JD000582.

Hamm, C.E., 2002. Interactive aggregation and sedimentation of diatoms and clay-sized lithogenic material. Limnology and Oceanography 47, 1790–1795.

Helmers, E., Rutgers van der Loeff, M.M., 1993. Lead and aluminum in Atlantic surface waters (50°N to 50°S) reflecting anthropogenic and natural sources in the aeolian transport. Journal of Geophysical Research 98, 20261–20273.

Hutchins, D.A., Bruland, K.W., 1994. Grazer-mediated regeneration and assimilation of Fe, Zn and Mn from planktonic prey. Marine Ecology. Progress Series 110, 259–269.

Hutchins, D.A., Witter, A.E., Butler, A., Luther, G.W., 1999. Competition among marine phytoplankton for different chelated iron species. Nature 400, 858–861.

Hydes, D.J., 1989. Seasonal variation in dissolved aluminium concentrations in coastal waters and biological limitation of the export of the riverine input of aluminium to the deep sea. Continental Shelf Research 9, 919–929.

Ittekkot, V., 1993. The abiotically driven biological pump in the ocean and short-term fluctuations in atmospheric CO_2 contents. Global and Planetary Change 8, 17–25.

Jickells, T.D., 1999. The inputs of dust derived elements to the Sargasso Sea; a synthesis. Marine Chemistry 68, 5–14.

Jickells, T.D., Spokes, L.J., 2001. Atmospheric Iron Inputs to the Oceans. In: Turner, D., Hunter, K. (Eds.), The Biogeochemistry of Iron in Seawater, IUPAC Book Series on Analytical and Physical Chemistry of Environmental Systems, vol. 7. John Wiley & Sons Ltd., Chichester, pp. 85–122.

Körtzinger, A., Hedges, J.I., Quay, P.D., 2001. Redfield ratios revisited: removing the biasing effect of anthropogenic CO_2. Limnology and Oceanography 46, 964–970.

Kramer, J., Laan, P., Sarthou, G., Timmermans, K.R., De Baar, H.J.W., 2004. Distribution of dissolved aluminium in the high atmospheric input region of the subtropical waters of the North Atlantic Ocean. Marine Chemistry 88, 85–101.

Kremling, K., 1985. The distribution of cadmium, copper, nickel, manganese and aluminium in surface waters of the open Atlantic and European shelf area. Deep-sea Research 32, 531–555.

Kremling, K., Hydes, D., 1988. Summer distribution of dissolved Al, Cd, Co, Cu, Mn and Ni in surface waters around the British Isles. Continental Shelf Research 8, 89–105.

Landing, W.M., Haraldsson, C., Paxeus, N., 1986. Vinyl polymer agglomerate based transition metal cation chelating ion-exchange resin containing the 8-hydroxyquinoline functional group. Analytical Chemistry 58, 3031–3035.

Landing, W.M., Measures, C.I., Buck, C.S., Brown, M., 2003. Sections of dissolved iron and aluminium from the 2003 repeat hydrography A16N expedition. EOS Transactions AGU 84(52), Ocean Sciences Supplement, Abstract OS31L-07.

Lohan, M., Aguilar-Islas, A.M., Bruland, K.W., 2006. Direct determination of iron in acidified (pH 1.7) seawater samples by flow injection analysis with catalytic spectrophotometric detection: application and intercomparison. Limnology and Oceanography-Methods 4, 164–171.

Mallini, L.M., Shiller, A.M., 1993. Determination of dissolved manganese in seawater by flow injection analysis with colorimetric detection. Limnology and Oceanography 38, 1290–1295.

Maranon, E., Behrenfeld, M.J., Gonzalez, N., Mourino, B., Zubkov, M.V., 2003. High variability of primary production in oligotrophic waters of the Atlantic Ocean: uncoupling from phytoplankton biomass and size structure. Marine Ecology. Progress Series 257, 1–11.

Martin, J.H., 1990. Glacial–interglacial CO_2 change: the iron hypothesis. Paleoceanography 5, 1–13.

Martin, J.H., Gordon, R.M., Fitzwater, S.E., 1991. The case for iron. Limnology and Oceanography 36, 1793–1802.

Measures, C.I., 1995. The distribution of Al in the IOC stations of the eastern Atlantic between 30°S and 34°N. Marine Chemistry 4, 267–281.

Measures, C.I., Brown, E.T., 1996. Estimating dust input to the Atlantic Ocean using surface water aluminium concentrations. In: Guerzoni, S., Chester, R. (Eds.), The Impact of Desert Dust across the Mediterranean. Kluwer Academic Publishers, The Netherlands, pp. 301–311.

Measures, C.I., Vink, S., 2000. On the use of dissolved aluminium in surface waters to estimate dust deposition to the ocean. Global Biogeochemical Cycles 14, 317–327.

Measures, C.I., Edmond, J.M., Jickells, T.D., 1986. Aluminium in the northwest Atlantic. Geochimica et Cosmochimica Acta 50, 1423–1429.

Minster, J.-F., Boulahdid, M., 1987. Redfield ratios along isopycnal surfaces—a complementary study. Deep-sea Research 34, 1981–2003.

Moran, S.B., Moore, R.M., 1988. Evidence from mesocosm studies for biological removal of dissolved aluminium from seawater. Nature 355, 706–708.

Moran, S.B., Moore, R.M., 1991. The potential source of dissolved aluminium from resuspended sediments to the North Atlantic Deep Water. Geochimica et Cosmochimica Acta 55, 2745–2751.

Moran, S., Moore, B., 1992. Kinetics of the removal of dissolved aluminium by diatoms in seawater: a comparison with thorium. Geochimica et Cosmochimica Acta 56, 3365–3374.

Obata, H., Karatani, H., Nakayama, E., 1993. Automated determination of iron in seawater by chelating resin concentration and chemiluminescence detection. Analytical Chemistry 65, 1524–1528.

Orians, K.J., Bruland, K.W., 1986. The biogeochemistry of aluminium in the Pacific Ocean. Earth and Planetary Science Letters 78, 397–410.

Poorvin, L., Rinta-Kanto, J.M., Hutchins, D.A., Wilhelm, S.W., 2004. Viral release of iron and its bioavailability to marine plankton. Limnology and Oceanography 49, 1734–1741.

Prospero, J.M., 1999. Long-term measurements of the transport of African mineral dust to the southeastern United States: implications for regional air quality. Journal of Geophysical Research 104 (D13), 15,917–15,928.

Resing, J., Measures, C.I., 1994. Fluorimetric determination of Al in seawater by FIA with in-line preconcentration. Analytical Chemistry 66, 4105–4111.

Sarthou, G., Baker, A.R., Blain, S., Achterberg, E.P., Boyé, M., Bowie, A.R., Croot, P., Laan, P., De Baar, H.J.W., Jickells, T.D., Worsfold, P.J., 2003. Atmospheric iron deposition and sea-surface concentrations in the eastern Atlantic Ocean. Deep-sea Research. Part 1. Oceanographic Research Papers 50, 1339–1352.

Schoemann, V., De Baar, H.J.W., De Jong, J.T.M., Lancelot, C., 1998. Effects of phytoplankton blooms on the cycling of manganese and iron in coastal waters. Limnology and Oceanography 43, 1427–1441.

Sedwick, P.N., Church, T.M., Bowie, A.R., Marsay, C.M., Ussher, S.J., Achilles, K.M., Lethaby, P.J., Johnson, R.J., Sarin, M.M., McGillicuddy, D.J., 2005. Iron in the Sargasso Sea (Bermuda Atlantic time-series study region) during summer: aeolian imprint, spatiotemporal variability, and ecological implications. Global Biogeochemical Cycles 19 (4), GB4006.

Spokes, L.J., Jickells, T.D., 1996. Factors controlling the solubility of aerosol trace metals in the atmosphere and on mixing into seawater. Aquatic Geochemistry 1, 355–374.

Sunda, W.G., 1997. Control of dissolved iron concentrations in the world ocean: a comment. Marine Chemistry 57, 169–172.

Takahashi, T., Broecker, W.S., Langer, S., 1985. Redfield ratio based on chemical data from isopycnal surfaces. Journal of Geophysical Research 90, 6907–6924.

Tappin, A.D., Hydes, D.J., Burton, J.D., Statham, P.J., 1993. Concentrations, distributions and seasonal variability of dissolved Cd, Co, Cu, Mn, Ni, Pb and Zn in the English Channel. Continental Shelf Research 13, 941–969.

Teira, E., Mourino, B., Maranon, E., Perez, V., Pazo, M.J., Serret, P., De Armas, D., Escanez, J., Woodward, E.M.S., Fernandez, E., 2005. Variability of chlorophyll and primary production in the Eastern North Atlantic Subtropical Gyre: potential factors affecting phytoplankton activity. Deep-sea Research. Part 1. Oceanographic Research Papers 52, 569–588.

Torres-Padrón, M.E., Gelado-Caballero, M.D., Collado-Sanchéz, C., Siruela-Matos, V.F., Cardona-Castellano, P.J., Hernández-Brito, J.J., 2002. Variability of dust inputs to the CANIGO zone. Deep-sea Research. Part 2. Topical Studies in Oceanography 49, 3455–3464.

Ussher, S.J., Bowie, A.R., Achterberg, E.P., Worsfold, P.J., 2006. Iron distribution and speciation along the Atlantic Meridional Transect (AMT). EOS Transactions AGU 87(36), Ocean Sciences Supplement, Abstract OS35M-18.

Van Aken, H.M., 2001. The hydrography of the mid-latitude Northeast Atlantic Ocean—part III: the subducted thermocline water mass. Deep-sea Research. Part 1. Oceanographic Research Papers 48, 237–267.

Van Bennekom, A.J., Buma, A.G.J., Nolting, R.F., 1991. Dissolved aluminium in the Weddell-Scotia Confluence and effect of Al on the dissolution kinetics of biogenic silica. Marine Chemistry 35, 423–434.

Veldhuis, M.J.W., Kraay, G.W., 2004. Phytoplankton in the subtropical Atlantic Ocean: towards a better assessment of biomass and composition. Deep-sea Research. Part 1. Oceanographic Research Papers 51, 507–530.

Wedepohl, K.H., 1995. The composition of the continental crust. Geochimica et Cosmochimica Acta 59, 1217–1232.

Wilhelm, S.W., Trick, C.G., 1995. Physiological profiles of *Synechococcus* (Cyanophyceae) in iron limiting continuous cultures. Journal of Phycology 31, 79–85.

Wilhelm, S.W., Maxwell, D.P., Trick, C.G., 1996. Growth, iron requirements, and siderophore production in iron-limited *Synechococcus* PCC7002. Limnology and Oceanography 41, 87–97.

Zubkov, M.V., Sleigh, M.A., Tarran, G.A., Burkill, P.H., Leakey, R.J.G., 1998. Picoplanktonic community structure on an Atlantic transect from 50°N to 50°S. Deep-sea Research 45, 1339–1355.